

# Water Resources Research®

## RESEARCH ARTICLE

10.1029/2024WR038199

## Revegetation Impacts on Moisture Recycling and Precipitation Trends in the Chinese Loess Plateau



### Key Points:

- Precipitation moisture source for Chinese Loess Plateau and its change were identified using a moisture tracking model
- The contribution of locally recycled moisture to Loess Plateau precipitation increased from 6.9% in 1982–1999 to 8.3% in 2000–2019
- Regional greening promotes precipitation by about 0.83 mm yr<sup>-1</sup>, while local vegetation accounts for about 0.07 mm yr<sup>-1</sup> during 2000–2019

### Supporting Information:

Supporting Information may be found in the online version of this article.

### Correspondence to:

W. Wang,  
wangweiguang@hhu.edu.cn

### Citation:

Cao, M., Wang, W., Wei, J., Forzieri, G., Fetzer, I., & Wang-Erlandsson, L. (2024). Revegetation impacts on moisture recycling and precipitation trends in the Chinese Loess Plateau. *Water Resources Research*, 60, e2024WR038199. <https://doi.org/10.1029/2024WR038199>

Received 13 JUN 2024

Accepted 20 NOV 2024

### Author Contributions:

**Conceptualization:** Mingzhu Cao, Weiguang Wang, Jia Wei, Ingo Fetzer, Lan Wang-Erlandsson

**Formal analysis:** Mingzhu Cao

**Funding acquisition:** Weiguang Wang

**Investigation:** Lan Wang-Erlandsson

**Methodology:** Mingzhu Cao,

Weiguang Wang, Jia Wei, Giovanni Forzieri, Ingo Fetzer, Lan Wang-Erlandsson





**Resources:** Weiguang Wang

**Software:** Mingzhu Cao

**Supervision:** Weiguang Wang, Ingo Fetzer, Lan Wang-Erlandsson

**Validation:** Mingzhu Cao

**Writing – original draft:** Mingzhu Cao

Mingzhu Cao<sup>1,2</sup>, Weiguang Wang<sup>1,2,3</sup> , Jia Wei<sup>1,2</sup> , Giovanni Forzieri<sup>4</sup> , Ingo Fetzer<sup>5,6</sup>, and Lan Wang-Erlandsson<sup>5,7,8</sup> 

<sup>1</sup>The National Key Laboratory of Water Disaster Prevention, Hohai University, Nanjing, China, <sup>2</sup>College of Hydrology and Water Resources, Hohai University, Nanjing, China, <sup>3</sup>Yangtze Institute for Conservation and Development, Hohai University, Nanjing, China, <sup>4</sup>Department of Civil and Environmental Engineering, University of Florence, Florence, Italy, <sup>5</sup>Stockholm Resilience Centre, Stockholm University, Stockholm, Sweden, <sup>6</sup>Bolin Centre for Climate Impact Research, Stockholm University, Stockholm, Sweden, <sup>7</sup>Anthropocene Laboratory, the Royal Swedish Academy of Sciences, Stockholm, Sweden, <sup>8</sup>Potsdam Institute for Climate Impact Research, Member of the Leibniz Association, Potsdam, Germany

**Abstract** The Loess Plateau in China has experienced a remarkable greening trend due to vegetation restoration efforts in recent decades. However, the response of precipitation to this greening remains uncertain. In this study, we identified and evaluated the main moisture source regions for precipitation over the Loess Plateau from 1982 to 2019 using a moisture tracking model, the modified WAM-2layers model, and the conceptual framework of the precipitation shed. By integrating multiple linear regression analysis with a conceptual hydrologically weighting method, we quantified the effective influence of different environmental factors for precipitation, particularly the effect of vegetation. Our analysis revealed that local precipitation has increased on average by 0.16 mm yr<sup>-1</sup> and evaporation by 5.17 mm yr<sup>-1</sup> over the period 2000–2019 after the initiation of the vegetation restoration project. Regional greening including the Loess Plateau contributed to precipitation for about 0.83 mm yr<sup>-1</sup>, among which local greening contributed for about 0.07 mm yr<sup>-1</sup>. Local vegetation contribution is due to both an enhanced local evaporation as well as an increased local moisture recycling (6.9% in 1982–1999; 8.3% in 2000–2019). Thus, our study shows that local revegetation had a positive effect on local precipitation, and the primary cause of the observed increase in precipitation over the Loess Plateau is due to a combination of local greening and circulation change. Our study underscores that increasing vegetation over the Loess Plateau has exerted strong influence on local precipitation and supports the positive effects for current and future vegetation restoration plans toward more resilient water resources managements.

## 1. Introduction

Large-scale vegetation restoration has emerged as one of the most effective measurements for ecosystem remediation and climate mitigation over the past few decades (Branch & Wulfmeyer, 2019; Doelman et al., 2019; Spracklen et al., 2018). Such land cover changes alter the surface characteristics and modify the exchange of energy and moisture between the land and the atmosphere (Bonan et al., 1992; Piao et al., 2019; Sterling et al., 2012; te Wierik et al., 2021). Newly established vegetation typically needs more water to grow and significantly increases the local evaporation over land (Wang et al., 2021). Thus, many revegetation efforts and forestation projects across the world, especially in water-limited areas, have been observed to reduce local water availability (Albaugh et al., 2013; Farley et al., 2005; Li et al., 2018; Spracklen et al., 2012). Precipitation, can also be impacted by revegetation through land-atmosphere interactions, through boundary-layer processes, moisture recycling, and circulation perturbation (Lawrence & Vandecar, 2015; Spracklen et al., 2018; Tuinenburg, 2013). Small-scale changes in land cover can produce strong gradients in surface flux on the atmosphere boundary layer. These changes in local thermodynamic profile subsequently can thermally and dynamically affect cloud formation, and convection, even mesoscale circulation (Garcia-Carreras & Parker, 2011; Khanna et al., 2017). Regional scale changes in land cover affect evaporation, which releases moisture to the atmosphere, and atmospheric circulation due to changes in the atmospheric heating gradient between land and ocean, thereby altering the water balance and moisture recycling (Spera et al., 2016; Spracklen et al., 2018). Understanding how precipitation responds to revegetation is, therefore, an important piece for understanding the overall hydrological impact of restoration projects.

© 2024. The Author(s).

This is an open access article under the terms of the [Creative Commons Attribution License](https://creativecommons.org/licenses/by/4.0/), which permits use, distribution and reproduction in any medium, provided the original work is properly cited.

**Writing – review & editing:**

Mingzhu Cao, Weiguang Wang, Jia Wei, Giovanni Forzieri, Ingo Fetzer, Lan Wang-Erlandsson

There is a growing recognition that impact of vegetation changes on precipitation also highly depend on where and the extent to which the moisture recycled from (Cui et al., 2022; Keys et al., 2019; Staal et al., 2018, 2020; Tuinenburg et al., 2022; van der Ent & Savenije, 2011; Wang-Erlandsson et al., 2018). To address the question of where and what extent evaporated moisture from source region returns as precipitation in sink region (Brubaker et al., 1993; Keys et al., 2012; Trenberth, 1999; van der Ent et al., 2010), atmospheric moisture tracking methods have rapidly developed over the latest decades. This methodological advancement has subsequently become a reliable foundation for mapping the effects of land-use change on precipitation (Baudena et al., 2021). As a result, the effects of anthropogenic revegetation in a specific area on precipitation can be isolated, while also considering the effects associated with spatial redistribution of recycled moisture through atmospheric transport.

The Grain for Green project, initiated by the Chinese government in 1999 on Chinese Loess Plateau to halt soil erosion - is one of the world's largest active revegetation programs (Feng et al., 2016). Over the past two decades, ecological restoration efforts have resulted in a visible “greening” trend across the Loess Plateau (Naeem et al., 2021; Yu et al., 2020). The large-scale vegetation restoration project brings about benefits such as soil erosion control, reduction in sediment yield, carbon storage, and an improvement in the quality of life for the 108 million people residing in the region (Feng et al., 2016; Hoek van Dijke et al., 2022; Liu et al., 2012; Wang et al., 2015). However, there is a growing concern regarding whether revegetation is detrimental to water availability in the long term (Feng et al., 2016; Liu et al., 2016). Previous studies have suggested that increased vegetation have caused a remarkable growth in evaporation, and further reduced the water availability in the semi-arid Loess Plateau (Jia et al., 2017; Liu et al., 2016; Zhang et al., 2018). Yet majority of the assessments neglect that precipitation can be mediated by vegetation through land-atmosphere feedbacks (Zhang et al., 2016). Many modeling studies have revealed that revegetation projects can enhance precipitation in dry areas (Achugbu et al., 2022; Liu et al., 2023; Wang, Zhang, et al., 2023; Wulfmeyer et al., 2014; Yosef et al., 2018). Moreover, past studies have shown an increase in local precipitation over the Loess Plateau in connection to the vegetation restoration (S. Chen, Xiong, et al., 2023; W. Chen, Xiong, et al., 2023; Liu et al., 2023; Lv et al., 2019; Tian et al., 2022; Zhang et al., 2022). However, uncertainties still exist as to whether such vegetation-driven increase in precipitation is large enough to compensate for evaporation losses. Analyses based on land-climate models, primarily the Weather Research and Forecasting (WRF) model and Land Surface Models (LSMs), account for both precipitation and evaporation change from revegetation, but are subject to uncertainties in biophysical parameterization schemes implemented in the models (de Noblet-Ducoudré et al., 2012; Forzieri et al., 2018; Ge et al., 2020). Thus, how precipitation on the Loess Plateau responds to revegetation or afforestation still lacks a consensus, and there is a necessity to disentangle restoration efforts' contribution based on observational evidence.

In this study, we address the following questions: (a) What changes have occurred in the different components of the atmospheric water cycle in the Loess Plateau over the last decades? (b) What contribution does the revegetation over the Loess Plateau make to local precipitation? We first identified the moisture source region (i.e., precipitationshed) of the precipitation over Loess Plateau by using the modified Water Accounting Model-2 layers (WAM-2layers) (Xiao & Cui, 2021), to help us separate the moisture contribution of local and remote sources. Then, we constructed a hydrologically effective leaf area index ( $LAI_w$ ) by weighting the satellite-observed leaf area index (LAI) with the moisture contribution of evaporation to precipitation over study area (Cui et al., 2022). This allows the hydrological connection between vegetation and precipitation to be detected at a regional scale, extending beyond the local level and encompassing upwind areas. Furthermore, a multiple linear regression model was adopted to disentangle the impacts of both local and remote vegetation changes on the local precipitation. Last, we discuss the underlying mechanisms for the changes in local precipitation following the revegetation project. Our study identifies the impact of restoration and revegetation efforts on improving local precipitation patterns over the Loess Plateau. By disentangling the factors influencing precipitation, in addition to climate change affecting the region, we provide valuable insights into the effectiveness of restoration and revegetation efforts. Outcomes of our research supports the integration of biophysical process into ecological restoration strategies, to ultimately foster the development of resilient water resources management, particularly in times of rapid climate change.

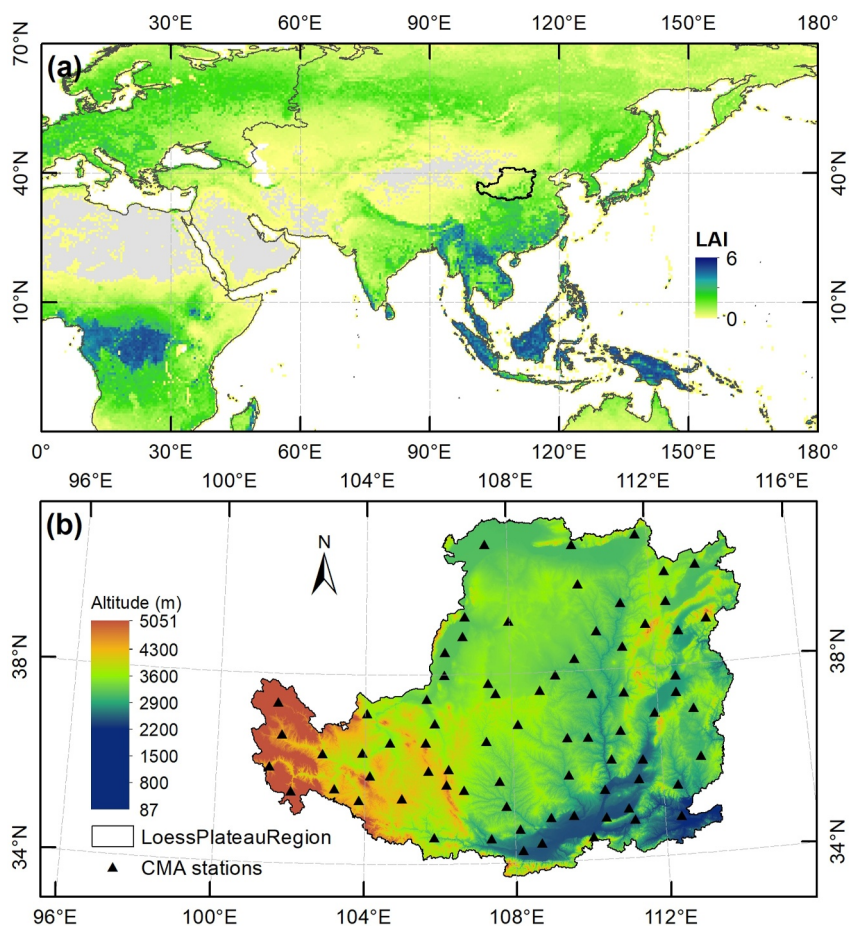


**Figure 1.** Location of the Loess Plateau. (a) The simulation domain which is the source area in our study. The color shading denotes the Leaf Area Index (LAI) ( $\text{m}^2 \text{m}^{-2}$ ) for 2018 from the GLASS data sets. (b) The topography of Loess Plateau which is the sink area. The black triangles show the locations of the China Meteorological Administration (CMA) stations.

## 2. Data and Methods

### 2.1. Study Area

The Loess Plateau ( $64,000 \text{ km}^2$ ) is located in the middle reaches of the Yellow River basin in northern China (Figure 1). The region spans arid, semi-arid, and semi-humid zones and is sensitive to climate change (Liu & Sang, 2013). The average annual temperature ranges from 6 to  $10^\circ\text{C}$  from northwest to southeast (Li et al., 2010). Meanwhile, it is a typical water-limited landscape with mean annual precipitation ranging from 200 to 800 mm, and the annual evaporation ranging from 150 to 600 mm, both computed over the 1982–2019 period. Controlled by the East Asian summer monsoon, about 70% of the precipitation concentrates in the rainy season (from June to September) (Tang et al., 2018). Due to the frequent rainstorms, steep landscapes, highly erodible soils, and low vegetation cover, the Loess Plateau has become one of the most ecologically vulnerable areas in China. To prevent soil erosion and improve local ecological conditions, the Chinese government has implemented the Grain for Green Project since 1999, which has led to a visible “greening” trend, with the vegetation cover increasing from 32% in 1999 to 64% in 2019 over the Loess Plateau (Wang, Fu, et al., 2023).

### 2.2. Data Set Collection

The satellite-based Leaf Area Index (LAI) generated by the Global Land Surface Satellites (GLASS) was used to analyze the vegetation cover conditions over the Loess Plateau ([https://doi.org/10.12041/geodata.GLASS\\_LAI\\_modis\(0.05D\).ver1.db](https://doi.org/10.12041/geodata.GLASS_LAI_modis(0.05D).ver1.db)). The GLASS LAI has a temporal resolution of 8 days and a spatial resolution of  $0.05^\circ$  (Liang, 2021). Data sets of LAI from Global Inventory Modeling and Mapping Studies (GIMMS), and the Long-

term Global Mapping LAI (GLOBMAP) were used for validation in this study. The GIMMS provides LAI twice a month with a spatial resolution of  $1/12^\circ$  (Cao et al., 2023), and the GLOBMAP provides the same temporal resolution and a spatial resolution of  $4/55^\circ$  (Liu et al., 2021). The Terra and Aqua combined Moderate Resolution Imaging Spectroradiometer (MODIS) Land Cover Climate Modeling Grid (CMG) (MCD12C1) Version 6.1 data product was used to capture land cover type change in the Loess Plateau from 2001 to 2019 (Friedl & Sulla-Menashe, 2022).

The input data sets used in the modified WAM-2layers model are specific humidity ( $Q$ ), surface pressure ( $SP$ ),  $u$ -velocity ( $U$ ), and  $v$ -velocity ( $V$ ) at 17 pressure levels (including 10, 100, 200, 300, 400, 500, 600, 700, 800, 825, 850, 875, 900, 925, 950, 975, and 1,000 hPa) and total column water at single level at 6-hr intervals from the fifth generation Earth Retrospective Analysis (ERA5) released by the European Center for Medium-Range Weather Forecasts (ECMWF) (Hersbach et al., 2020). In addition, precipitation ( $P$ ) data were acquired at 3-hr intervals from the Multi-Source Weighted-Ensemble Precipitation (MSWEP) (Beck et al., 2017) and evaporation ( $E$ ) at 1-hr intervals from the Modern-Era Retrospective analysis for Research and Applications, version 2 (MERRA-2) (GMAO, 2015a) at single level.

Daily precipitation was validated with in-situ observation from China Meteorological Administration (CMA) at 74 stations in the Loess Plateau (<http://data.cma.cn/>). In addition, the monthly  $P$  during 1982–2018 at  $0.1^\circ$  resolution from the China Meteorological Forcing Data set (CMFD) (Yang et al., 2019), the monthly  $P$  during 1982–2019 at  $0.5^\circ$  resolution from the Climate Prediction Center (CPC) Unified Precipitation Project (Chen et al., 2008) (<https://psl.noaa.gov>), the monthly  $P$  during 1982–2019 at  $0.5^\circ$  resolution from Climatic Research Unit Time series version 4 (CRU TS4.0) (Harris et al., 2020) (<https://crudata.uea.ac.uk/cru/data/hrg/>), and the monthly  $P$  during 1982–2019 at  $0.5^\circ$  resolution from Global Precipitation Climatology Center (GPCC) (Schneider et al., 2015) (<https://psl.noaa.gov/data/gridded/data.gpcc.html>) were used for comparison in our study. Monthly gridded  $P$  from MSWEP agrees well with the observed  $P$  from CMA (Figure S1 in Supporting Information S1), with an averaged correlation strength of Pearson's  $R = 0.88$  for all stations, supporting the validity and accuracy of the MSWEP  $P$  over the Loess Plateau. The year 1992 was omitted from the analysis in our study, since MSWEP  $P$  shows an anomaly in 1992 when compared to the other products (Figure S2 in Supporting Information S1).

Similarly, the following products were used in this study for the comparison of evaporation: monthly total Latent Energy Flux during 1982–2019 from MERRA2 at  $0.625^\circ \times 0.5^\circ$  resolution (GMAO, 2015b); 8d Evapotranspiration during 1982–2018 from Global Land Surface Satellite (GLASS) at  $0.05^\circ$  resolution (Yao et al., 2014); monthly Actual Evaporation during 1982–2019 from Global Land Evaporation Amsterdam Model (GLEAM) at  $0.1^\circ$  resolution (Miralles et al., 2011); monthly Evapotranspiration from Breathing Earth System Simulator (BESS) at  $0.5^\circ$  resolution covering the periods from 1982 to 2014, 2015, 2016 retrieved by GLASS, GIMMS, GLOBMAP LAI respectively (Jiang & Ryu, 2016); monthly Latent Heat Flux during 2001–2013 from Fluxcom at  $0.5^\circ$  resolution (Jung et al., 2019) (<https://www.bgc-jena.mpg.de/geodb/projects/Home.php>). As shown in Figure S3 in Supporting Information S1, the regional averaged  $E$  over the Loess Plateau from ERA5 is lower than those from other products. Meanwhile, the ERA5  $E$  exhibits a decreasing trend, which differs from the others. Hence, the MERRA2  $E$  data was chosen as in the absence of observation from eddy covariance tower, it can meet the resolution requirements of the model and close the terrestrial water budget over the Loess Plateau (Tian et al., 2022).

In addition, six monthly climatic variables and large climate variability indices on El Niño/Southern Oscillation (ENSO) and Indian Ocean Dipole (IOD) were adopted for analysis in this study. The six climatic variables such as 10 m  $u$ -component of wind ( $U$ ), 10 m  $v$ -component of wind ( $V$ ), 2 m temperature ( $T_a$ ), 2 m dewpoint temperature ( $T_d$ ), surface pressure ( $SP$ ), surface net solar radiation (SSR), Surface net thermal radiation (STR) and Volumetric soil water layer 1–3 (SM) are provided by ERA5 (Hersbach et al., 2020). The climate variability indices used in our study are Niño3.4 SST Index (hereinafter referred to as NINO) ([https://psl.noaa.gov/gcos\\_wgsp/Timeseries/Nino34/](https://psl.noaa.gov/gcos_wgsp/Timeseries/Nino34/)) and Dipole Mode Index (DMI) ([https://psl.noaa.gov/gcos\\_wgsp/Timeseries/DMI/](https://psl.noaa.gov/gcos_wgsp/Timeseries/DMI/)). ENSO and IOD were selected for their strong influence on precipitation patterns over the Loess Plateau. Statistical analysis further supported their relevance, showing that ENSO is a major influencing factor, while IOD, although less critical, still holds importance among the climate variabilities analyzed (Tables S1, and S2 in Supporting Information S1).

To assess the water budget, annual runoff observations from 2000 to 2019 were obtained from the Ministry of Water Resources of the People's Republic of China (<http://www.mwr.gov.cn/sj/tjgb/szygb/>), soil moisture

content was acquired from Global Land Data Assimilation System (GLDAS) (Beaudoin et al., 2020) and Terrestrial Water Storage data was derived from previous research (S. Chen, Xiong, et al., 2023; W. Chen, Xiong, et al., 2023). Detailed information of the data sets used in this study are summarized Table S3 in Supporting Information S1.

### 2.3. Moisture Tracking Method

Our study used the modified Water Accounting Model-2 layers (WAM-2layers) to track the atmospheric moisture (Xiao & Cui, 2021). The WAM-2Layers model is a Eulerian model on moisture recycling, which can track moisture either forward or backward in time to quantify the moisture source-sink relations (van der Ent et al., 2010, 2014). The WAM-2layers model divides the zero pressure to surface pressure into two layers. Within these layers, atmospheric moisture is assumed to be well mixed. The underlying principle is the atmospheric water balance (van der Ent et al., 2014):

$$\frac{\partial S_k}{\partial t} = \frac{\partial(S_k u_k)}{\partial x} + \frac{\partial(S_k v_k)}{\partial y} + E_k - P_k + \sigma_k \pm F_v \quad [m^3] \quad (1)$$

where  $S_k$  refers to atmospheric moisture storage in layer  $k$  (the top or bottom layer);  $E$  refers to evaporation;  $P$  refers to precipitation;  $u$  and  $v$  refer to wind speed in the zonal and meridional direction, respectively;  $\sigma$  refers to residual; and  $F_v$  refers to vertical moisture transport. For each grid cell, total evaporation is denoted as  $E$ , and the evaporation that passes through the atmosphere and falls as precipitation over the Loess Plateau is denoted  $E_r$ . For grid at location  $(i, j)$ , the grid cell evaporation recycling ratio ( $\varepsilon_{i,j}$ ) and the grid cell contribution ratio expressing as the contribution of the grid cell evaporation to the precipitation over the Loess Plateau ( $\omega_{i,j}$ ) are defined as follows (van der Ent et al., 2010).

$$\varepsilon_{i,j} = \frac{E_{r,i,j}}{E_{i,j}} \quad (2)$$

$$\omega_{i,j} = \frac{E_{r,i,j}}{P_{LP}} \quad (3)$$

Thus, for the entire Loess Plateau (LP), the locally recycled moisture ( $ER_{LP}$ ), the moisture evaporated from the Loess Plateau and landed on the downwind areas outside the plateau ( $E_{out}$ ), the local evaporation recycling ratio ( $\varepsilon_{LP}$ ) and the local contribution ratio ( $\omega_{LP}$ ) are defined as follows (van der Ent et al., 2010) (Figure 2 STEP 1).

$$ER_{LP} = \sum_{i,j \in LP} E_{r,i,j} \quad (4)$$

$$E_{out} = E_{LP} - ER_{LP} \quad (5)$$

$$\varepsilon_{LP} = \frac{ER_{LP}}{E_{LP}} \quad (6)$$

$$\omega_{LP} = \frac{ER_{LP}}{P_{LP}} \quad (7)$$

The spatial resolution of the modified WAM-2layers model in this study is  $0.5^\circ$  and input data were linearly interpolated to the 10 min time step to maintain numerical stability. Our study is limited to a regional scope, and the simulation domain spans from  $0^\circ$  to  $180^\circ E$  and from  $20^\circ S$  to  $70^\circ N$ . With the study period being 1982–2019, the year 2020 is used as spin-up for backward tracking in WAM-2layers. Based on the original Python code forced by ERA-Interim data (<https://github.com/ruudvdent/WAM2layersPython>), Xiao and Cui (2021) modified the code to fit the ERA5 data and shared it at GitHub (<http://doi.org/10.5281/zenodo.4796962>).

Based on the output of the modified WAM-2layers model, the conceptual framework of precipitationshed (Keys et al., 2012, 2014) is taken to identify the main moisture source region for the Loess Plateau precipitation. In this study, the precipitationshed refers to the area that supplies 70% of the total evaporation to the Loess Plateau.

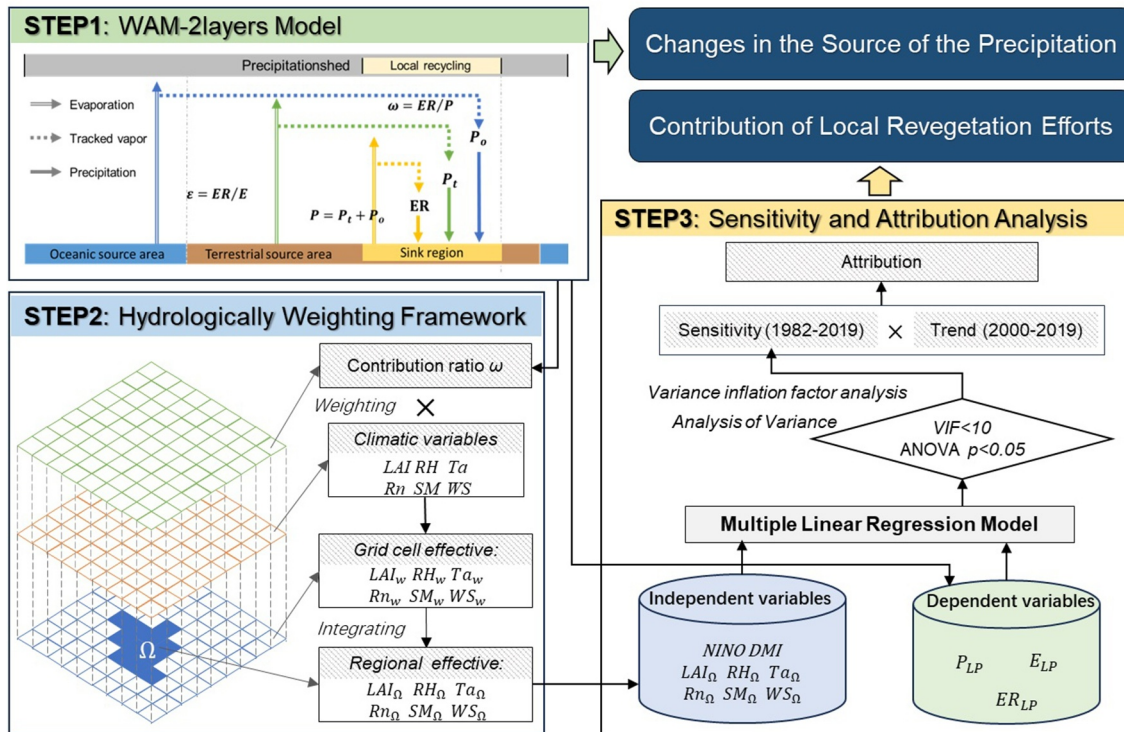


**Figure 2.** The conceptual diagram for this study. The flowchart of this study. P, Precipitation; E, Evaporation; ER, Local recycled moisture;  $P_o$ , Precipitation originated from oceanic sources;  $P_t$ , Precipitation originated from terrestrial sources;  $\epsilon$ , Evaporation recycling ratio;  $\omega$ , Contribution ratio; LAI, Leaf Area Index; RH, Relative humidity; Ta, Air temperature; Rn, Net radiation; SM, Soil moisture; WS, Wind speed; NINO, Niño3.4 SST Index; DMI, Dipole Mode Index; LP, Loess Plateau.

### 2.4. Hydrologically Weighting Analysis

To more accurately reflect the physical processes driving changes in the hydrological cycle of the Loess Plateau, we introduced a new conceptual hydrological weighting method (Figure 2 STEP 2). Our method is inspired by Cui et al. (2022), who accounted for the contribution of vegetation by integrating the monthly effective LAI values within the precipitationshed. The effective LAI captures the hydrological connection between vegetation to moisture sink area by weighting LAI in each grid cell with its moisture contribution to local precipitation. First, grid cells were weighted based on their significance, which is its relative contribution to the target area precipitation in this study. Then, the grid cell information was integrated into representative regional information at different scales. Thus, this approach ensures that the influence of regional environmental factors on precipitation over the Loess Plateau can be quantified more accurately. The hydrologically effective value of different variables in each grid cell was defined as:

$$X_{w,i,j} = \omega_{i,j} \times X_{i,j}, \quad (8)$$

in which,  $X$  represents any of the environmental factors included in our study, namely LAI, relative humidity (RH), air temperature (Ta), net radiation (Rn), soil moisture (SM) and windspeed (WS). The equation can be applied to understand the local effective  $X_{LP}$  and regional effective  $X_{all}$  contribution (“region” here refers to the simulated domain, i.e. 0°–180°E, 20°S–70°N) of the environmental factors as follows.

$$X_{LP} = \sum_{i,j}^{i,j \in LP} X_{w,i,j} \quad (9)$$

$$X_{all} = \sum_{i,j}^{i,j \in all} X_{w,i,j} \quad (10)$$

here, to differentiate with  $X_{LP}$ , the regional averaged value is shown as  $\overline{X_{LP}}$

$$\overline{X_{LP}} = \sum_{ij}^{i,j \in LP} X_{ij}/N \quad (11)$$

in which, N is the number of grid cells that belong to the Loess Plateau.

### 2.5. Sensitivity and Attribution Analysis

In this study, we applied the methodology described in Forzieri et al. (2017, 2020) to explore the interplay between the environmental factors and hydrological changes within a multiple linear regression framework (Figure 2 STEP 3). In order to isolate the effect of LAI from potential confounding effects, climatic indices and environmental factors, including NINO, DMI, LAI, RH, Ta, Rn, SM and WS, were initially included as independent predictors. While the hydrological terms (i.e.,  $P_{LP}$ ,  $ER_{LP}$  and  $E_{LP}$ ) are served as the dependent variables in the regression model. Subsequently, the sensitivity was expressed as the partial derivative resulted from a multiple linear regression analysis. Here, the sensitivity of Loess Plateau  $P$  was calculated as the partial derivative in the multiple regression of precipitation against predictors such as NINO, DMI, and the regional effective LAI<sub>All</sub>, RH<sub>All</sub>, Ta<sub>All</sub>, Rn<sub>All</sub>, SM<sub>All</sub> and WS<sub>All</sub>. In this study, the sensitivity is initially calculated at annual, rainy season and dry season scales for the period from 1982 to 2019. We refer to the rainy season as the months from June to September, and the dry season as the remaining months (S. Chen, Xiong, et al., 2023; W. Chen, Xiong, et al., 2023). The analytical formulation for the sensitivity analyses is as follows:

$$P_{LP} = \beta_0 + \frac{\partial P_{LP}}{\partial NINO} NINO + \frac{\partial P_{LP}}{\partial DMI} DMI + \frac{\partial P_{LP}}{\partial LAI_{All}} LAI_{All} + \frac{\partial P_{LP}}{\partial RH_{All}} RH_{All} + \frac{\partial P_{LP}}{\partial Ta_{All}} Ta_{All} + \frac{\partial P_{LP}}{\partial Rn_{All}} Rn_{All} + \frac{\partial P_{LP}}{\partial SM_{All}} SM_{All} + \frac{\partial P_{LP}}{\partial WS_{All}} WS_{All} \quad (12)$$

$$ER_{LP} = \beta_0 + \frac{\partial ER_{LP}}{\partial NINO} NINO + \frac{\partial ER_{LP}}{\partial DMI} DMI + \frac{\partial ER_{LP}}{\partial LAI_{LP}} LAI_{LP} + \frac{\partial ER_{LP}}{\partial RH_{LP}} RH_{LP} + \frac{\partial ER_{LP}}{\partial Ta_{LP}} Ta_{LP} + \frac{\partial ER_{LP}}{\partial Rn_{LP}} Rn_{LP} + \frac{\partial ER_{LP}}{\partial SM_{LP}} SM_{LP} + \frac{\partial ER_{LP}}{\partial WS_{LP}} WS_{LP} \quad (13)$$

$$E_{LP} = \beta_0 + \frac{\partial E_{LP}}{\partial NINO} NINO + \frac{\partial E_{LP}}{\partial DMI} DMI + \frac{\partial E_{LP}}{\partial LAI_{LP}} LAI_{LP} + \frac{\partial E_{LP}}{\partial RH_{LP}} RH_{LP} + \frac{\partial E_{LP}}{\partial Ta_{LP}} Ta_{LP} + \frac{\partial E_{LP}}{\partial Rn_{LP}} Rn_{LP} + \frac{\partial E_{LP}}{\partial SM_{LP}} SM_{LP} + \frac{\partial E_{LP}}{\partial WS_{LP}} WS_{LP} \quad (14)$$

where each term  $\frac{\partial Z}{\partial X}$  represents the sensitivity of the Z target variable to the X predictor variable. In particular,  $\frac{\partial P_{LP}}{\partial LAI_{All}}$ ,  $\frac{\partial ER_{LP}}{\partial LAI_{LP}}$ , and  $\frac{\partial E_{LP}}{\partial LAI_{LP}}$  are the sensitivity of  $P_{LP}$ ,  $ER_{LP}$  and  $E_{LP}$  to effective LAI changes.

Given the collinearity among the candidate variables and the insignificant performance of the full-factor regression model, it is necessary to filter the candidate variables. However, through our attempts, we found that it was impossible to obtain an ideal regression model due to the complex relationships among the variables. Therefore, we chose to develop regression models using different combinations of independent variables that meet several criteria, generating a range of the sensitivity analysis results, rather than relying on a single value. Variance inflation factor analysis (VIF < 10) and Analysis of Variance (ANOVA) method (with  $p < 0.05$ ), were conducted to assess the potential collinearity among predictors and the significance of the model (Gonsamo et al., 2021).

Variations in hydrological terms attributed to long-term changes in environmental factors were thus calculated by multiplying the sensitivity term with the trend of the variables from 2000 to 2019 (Chen et al., 2022; Forzieri et al., 2017, 2020). Using the LAI as an example, the formulas are as follows.

$$\delta P_{LP}^{LAI_{All}} = \frac{\partial P_{LP}}{\partial LAI_{All}} \times \delta LAI_{All} \quad (15)$$

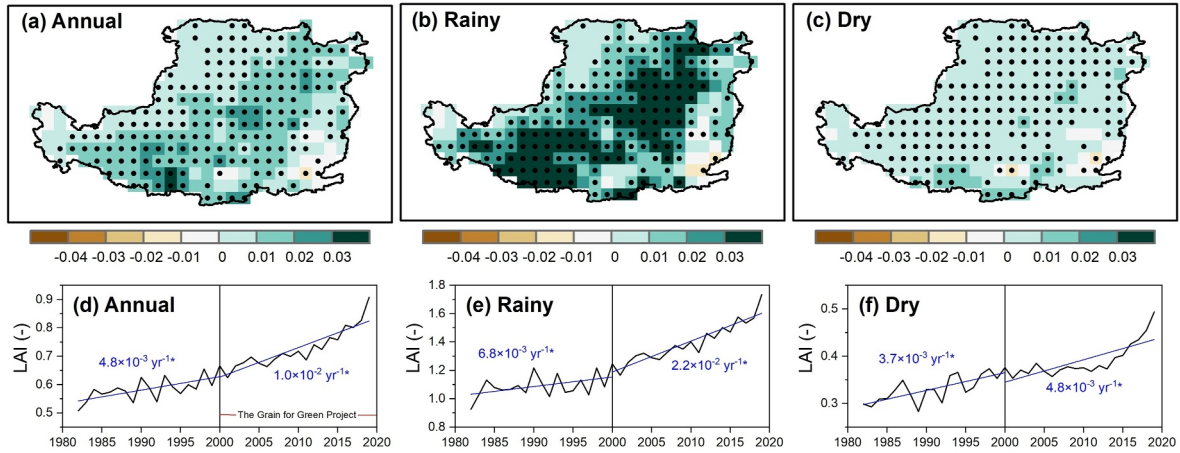


**Figure 3.** Spatial distribution of (a–c) the linear trend of averaged LAI for the annual, rainy season, and dry season after the Grain for Green Project (2000–2019), and (d–f) time series of regional averaged LAI over the entire Loess Plateau. Black dots and stars indicate that the trend is significant (Mann-Kendall test,  $p$ -value < 0.05).

$$\delta ER_{LP}^{LAI_{LP}} = \frac{\partial ER_{LP}}{\partial LAI_{LP}} \times \delta LAI_{LP} \quad (16)$$

$$\delta E_{LP}^{\overline{LAI}_{LP}} = \frac{\partial E_{LP}}{\partial \overline{LAI}_{LP}} \times \delta \overline{LAI}_{LP} \quad (17)$$

For the trend of the LAI ( $\delta LAI$ ), we performed Linear Least Squares Regression analysis as a trend analysis in a time series. Thus,  $\delta P_{LP}^{LAI_{All}}$ ,  $\delta ER_{LP}^{LAI_{LP}}$ , and  $\delta E_{LP}^{\overline{LAI}_{LP}}$  refer to the variations in local precipitation, recycled moisture and evaporation associated with the long-term changes in LAI. Since no model could meet the criteria, the attribution of annual  $P_{LP}$  was calculated as the sum of its attribution for the rainy and dry seasons.

## 2.6. Stepwise Selection Method for Factor Significance Detection

In addition, we performed the Forward and Backward Stepwise Selection to detect the significance of potential environmental factor combinations on hydrological terms (i.e.,  $P_{LP}$ ,  $ER_{LP}$  and  $E_{LP}$ ) (Chambers & Hastie, 1992; Venables & Ripley, 2002). The overall significance of the regression model was tested by an ANOVA, and the variables were added or removed according to the resulting new  $p$ -value in comparison with the previous model.

## 3. Results

In the following, we first present the trends of the vegetation over the Loess Plateau in Section 3.1. Then we investigated the trends of the local moisture recycling in Section 3.2, and the moisture source and their changes of the precipitation in Section 3.3. Finally, we quantified the effects of the revegetation on precipitation in Section 3.4.

### 3.1. Changes in Vegetation

The Loess Plateau has experienced a widespread greening over the past 38 years (1982–2019). As shown in Figure 3, LAI for the entire Loess Plateau increased significantly from 0.51 (1982) to 0.91 (2019). Mean increase rate  $0.0076 \text{ years}^{-1}$  at the annual time scale, and higher in the rainy season ( $0.0160 \text{ years}^{-1}$ ) and lower in the dry season ( $0.0035 \text{ years}^{-1}$ ). We found a significant increase in mean annual LAI over 76% of the areas on the Loess Plateau (Figure 3). The greening trend has increased dramatically after the implementation of the Grain for Green Project. Especially for mean LAI in rainy season, the changing rate grown from  $0.0068 \text{ years}^{-1}$  to  $0.022 \text{ years}^{-1}$ . In addition to the regional averaged LAI ( $\overline{LAI}_{LP}$ ), the local and regional effective LAIs ( $LAI_{All}$  and  $LAI_{LP}$ ) exhibited similar increasing trends, which were validated by the GIMMS and GLOBMAP products as well (Figure S4 in Supporting Information S1). Meanwhile, by comparing the land cover type between 1982 and 2019, we found that 6.98% of the Loess Plateau area has been converted from other land use types to grassland, 10.05%



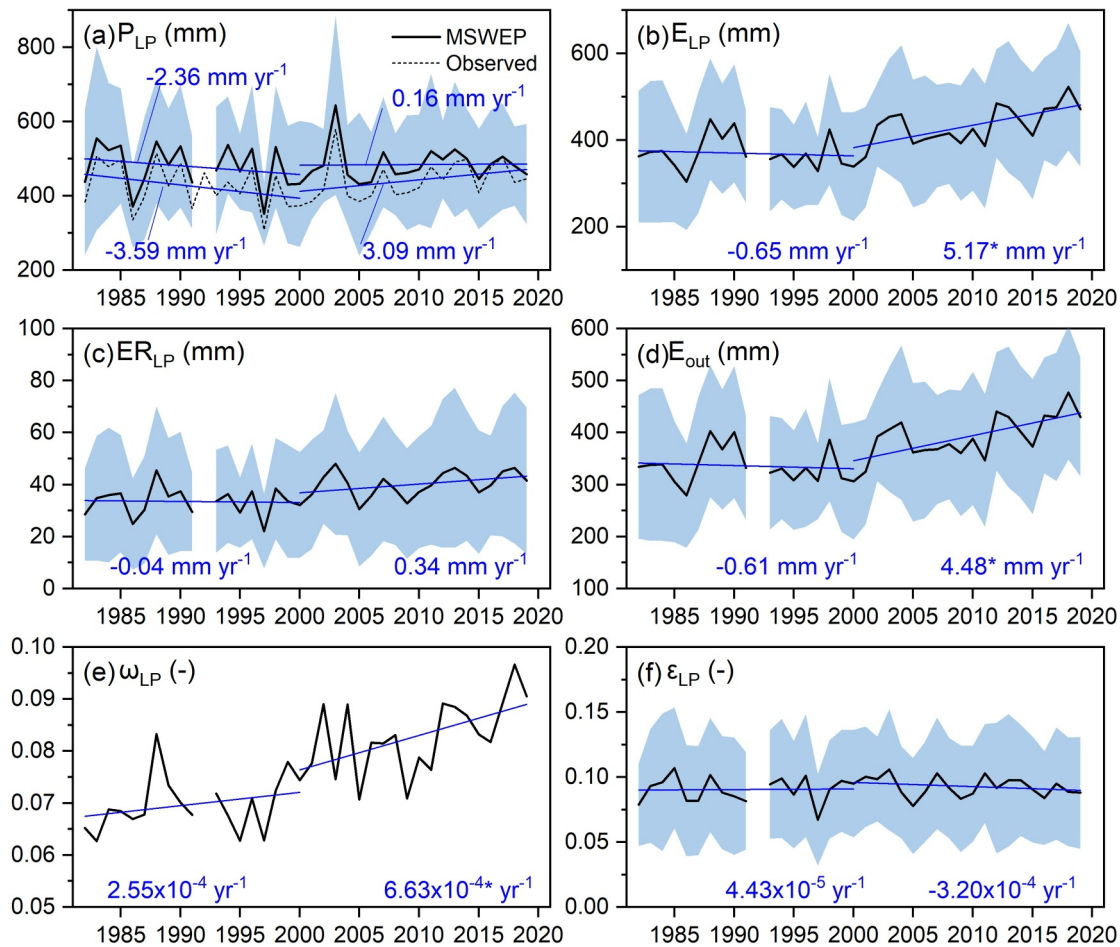


**Figure 4.** Time series of regional averaged (a) precipitation ( $P_{LP}$ ), (b) evaporation ( $E_{LP}$ ), (c) locally recycled moisture ( $ER_{LP}$ ), (d) evaporation that flows out of the Loess Plateau ( $E_{out}$ ), (e) contribution ratio ( $\omega_{LP}$ ) and (f) evaporation recycling ratio ( $\epsilon_{LP}$ ) for the entire Loess Plateau. Blue lines represent trends before and after the Grain for Green Project (none of them are significant). Shaded areas denote the spatial standard deviation. Star indicates that the trend is significant. The year 1992 was removed from the time series in this study, because the precipitation data for that year were anomalous high (Figure S2 in Supporting Information S1).

to cropland, and 1.33% from grassland to forest (Figure S5 in Supporting Information S1). Moreover, the greening trend is more pronounced in the central part of the Plateau and in the rainy season.

### 3.2. Changes in Moisture Recycling

When  $P$  and  $E$  are spatially aggregated over the Loess Plateau, they show a transition from decreasing trends to increasing trends after year 2000. The mean annual precipitation over the Loess Plateau ( $P_{LP}$ ) increased by about 2.7 mm, and the mean annual evaporation ( $E_{LP}$ ) by about 60.6 mm (Figures 4a and 4b). Though insignificant, the annual  $P_{LP}$  declined substantially at a rate of  $-2.36 \text{ mm yr}^{-1}$  during 1982–2000, and had a positive rate of  $0.16 \text{ mm yr}^{-1}$  for 2000–2019. Similarly, the changing rate of the annual  $E_{LP}$  is reversed from a decreasing trend of  $-0.65 \text{ mm yr}^{-1}$  to an increasing trend of  $5.17 \text{ mm yr}^{-1}$  during the same period. Spatially, the increase of  $P$  was concentrated in central part of the Loess Plateau, while  $E$  increased over most area and was more intense over the central-south and west regions after 2000, which in turn led to a decline in the water budget in the southern Loess Plateau (Figure S6 in Supporting Information S1).

The local moisture recycling was then analyzed to better elucidate the impacts of local vegetation restoration. On average, annual locally recycled moisture ( $ER_{LP}$ ) was 37.02 mm and accounted for 7.7% of local precipitation (Figures 4c and 6a). As shown in Figures 4c–4f, the  $ER_{LP}$  changed at the rate of  $-0.05$  and  $0.34 \text{ mm yr}^{-1}$  before and after 2000. Although both are increasing, the trend in the local contribution ratio ( $\omega_{LP}$ ), after 2000 was much sharper after the year 2000 than before. Meanwhile,  $E_{out}$  increased at the rate of  $4.48 \text{ mm yr}^{-1}$  after 2000,

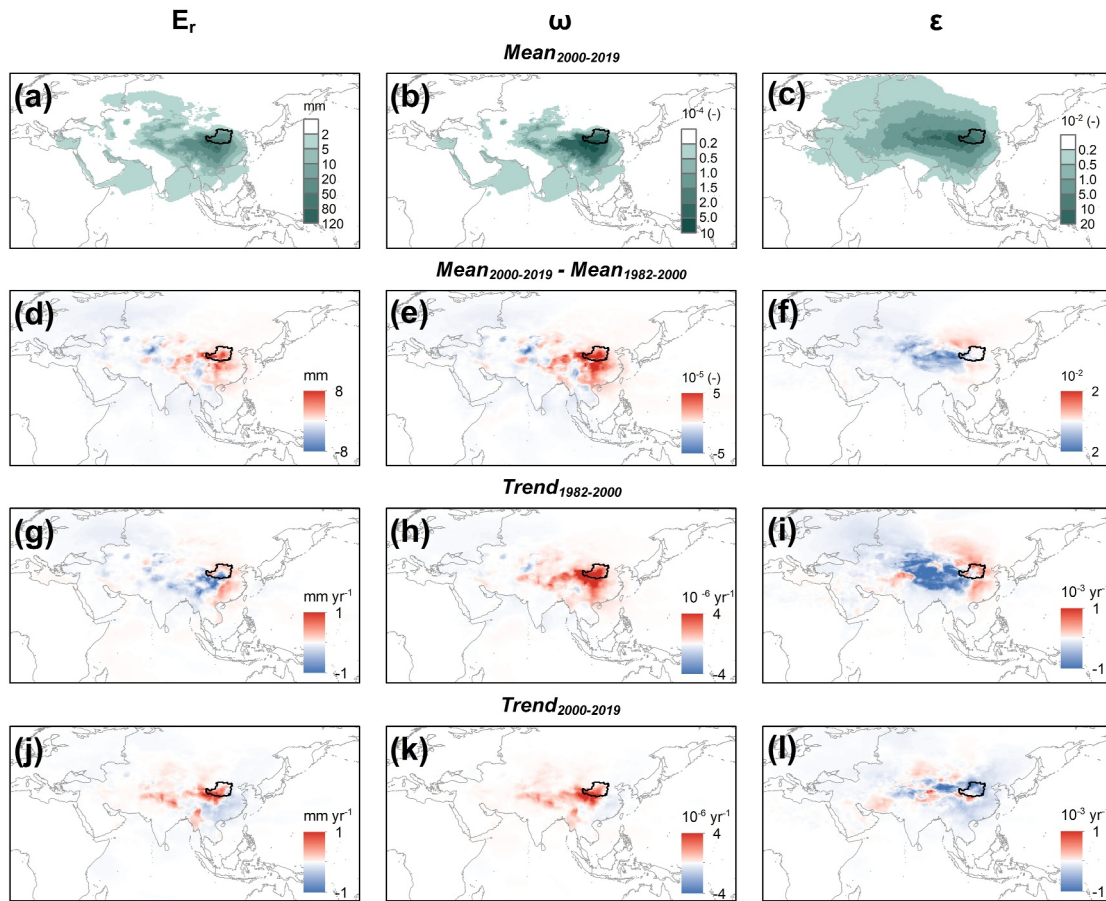


**Figure 5.** Spatial distribution of (a–c) mean annual recycled moisture ( $E_r$ ), contribution ratio ( $\omega$ ), and evaporation recycling ratio ( $\epsilon$ ) during 2000–2019; (d–f) the difference in mean annual  $E_r$ ,  $\omega$ , and  $\epsilon$  before and after the project; (g–i) the linear trend of  $E_r$ ,  $\omega$ , and  $\epsilon$  during 1982–2000; (j–l) the linear trend of  $E_r$ ,  $\omega$ , and  $\epsilon$  during 2000–2019.

continuously replenishing moisture to the downwind areas outside the Loess Plateau. Furthermore, the trend of the local evaporation recycling ratio ( $\epsilon_{LP}$ ) had an increasing trend during 1982–2000, and reversed to a decreasing trend during 2000–2019; however, both trends were shown to be insignificant. This transition suggests that although the absolute amount of local moisture contributing to local precipitation increased after 2000, a higher proportion of moisture evaporated from the Loess Plateau contributes to precipitation outside the region. Comparing the trend of  $E_{LP}$  with that of  $E_{out}$ , it becomes apparent that the change in  $E$  in the Loess Plateau has had a greater impact on the precipitation in downwind areas than within the plateau (Figure S7 in Supporting Information S1).

Generally, the annual moisture contribution indicated that the influence from the south is substantial and intense, while the influence from the west is mild but extensive (Figures 5a, 5b, 6a, and 6c). High contribution moisture sources are mainly distributed in the Loess Plateau itself and in central China south of the Loess Plateau. As shown in Figures 6b and 6c, moisture from the Indian Ocean is more important in the rainy season than dry season. Overall, more precipitation over the Loess Plateau originated from the continents (66.5%) than from the ocean (25.3%). The remaining 8.2% of the moisture comes from the region outside our simulation domain. Compared to the dry season, the rainy season had a higher proportion of local moisture in precipitation, a lower proportion of moisture from land outside the Loess Plateau, and a similar proportion of moisture from the ocean (Figures 6b and 6c).

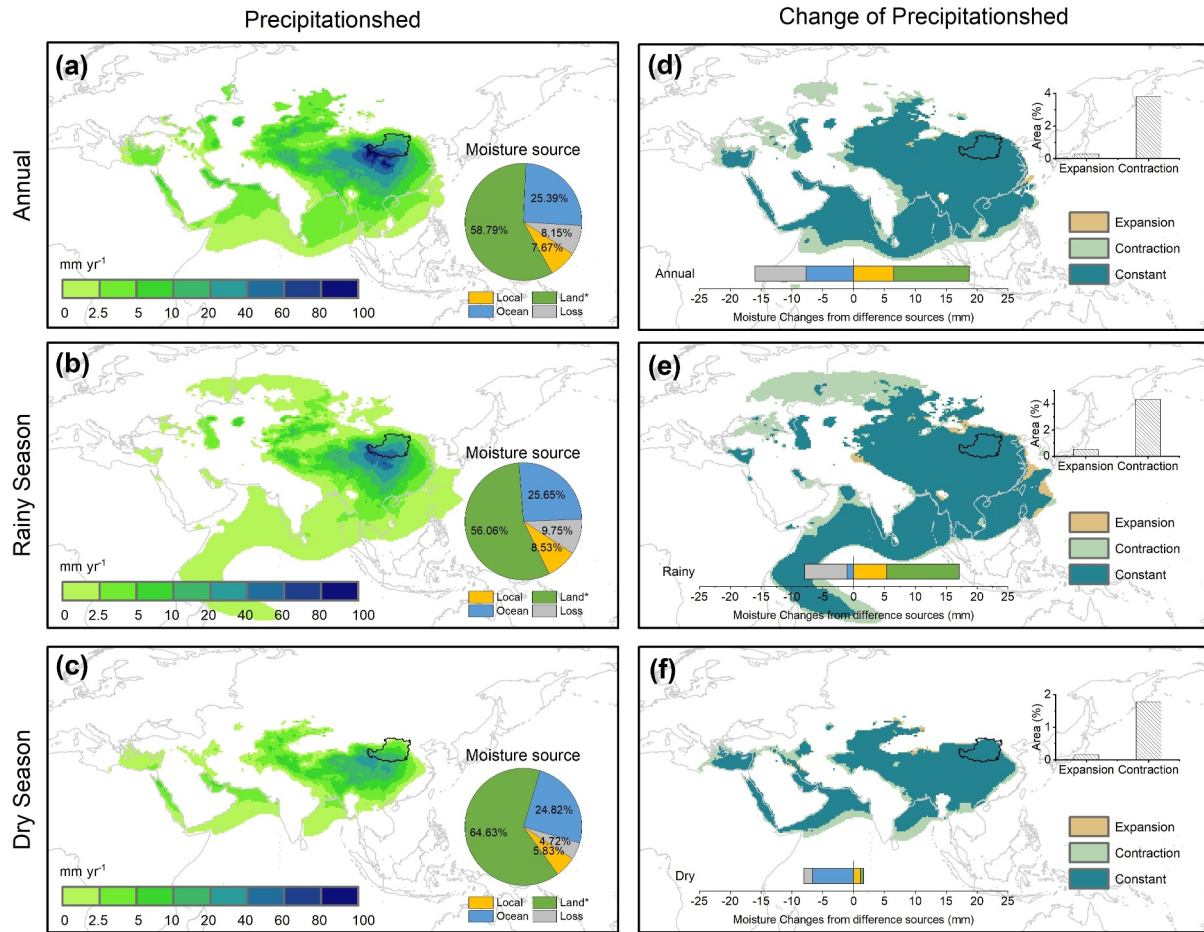


**Figure 6.** Precipitationsheds of (a–c) the annual, rainy season and dry season during 1982–2019. The pie charts show the percentage of different moisture sources. (d–f) The difference in precipitationsheds before and after the project. Bars on the right display the area change of the precipitationsheds, and bars at the bottom show the changes of the moisture from different sources that comprise precipitation on the Loess Plateau before and after the project (land\* means land excluding the Loess Plateau).

### 3.3. Changes in Moisture Sources of Loess Plateau Precipitation

We compared the moisture sources between 1982–1999 and 2000–2019 to explore the changes in precipitation composition over the Loess Plateau. The difference in mean annual precipitation before and after 2000 was 2.7, 9.2 and  $-6.4$  mm for the whole year, rainy season and dry season, respectively. Figure 6d shows that the increase of precipitation is mainly due to land. Comparing the changes in moisture from different sources in Figures 6e and 6f, the increase in precipitation was mainly concentrated in the rainy seasons. After 2000, annual  $P$  originated from the Loess Plateau was 6.5 mm higher than before and in the rainy season, it was 5.4 mm higher. The difference in moisture from the land outside the Loess Plateau was 12.2 mm for the whole year and 11.8 mm for the rainy season. During the dry season, the ocean generally played a negative role, with a change of  $-6.6$  mm.

In most areas over the Loess Plateau,  $E_r$  and the contribution ratio  $\omega$  increased, while the change in evaporation recycling ratio  $\epsilon$  was very slight.  $E_r$  showed a spatial pattern of increase in the south and decrease in the remote west after 2000, while  $\epsilon$  declined obviously over the Tibetan Plateau (Figures 5d–5f). As shown in Figures 5g–5l,  $E_r$  experienced an abrupt increasing trend during 2000–2019, especially in central and southwest part of the Loess Plateau, in contrast with the downward trend during 1982–2000. Moreover,  $\omega$  exhibited a similar trend to  $E_r$  after 2000, and had an increasing trend in most areas before the implementation of the project. Furthermore, the evaporation recycling ratio  $\epsilon$  had an increasing trend over the most areas of the Loess Plateau before, while experienced a decreasing trend during 2000–2019.

**Table 1**  
The Correlation Coefficient Between Hydrology Terms and the Environmental Factors

R		<i>NINO</i>	<i>DMI</i>	$LAI_{All}$	$RH_{All}$	$Ta_{All}$	$Rn_{All}$	$SM_{All}$	$WS_{All}$
$P_{LP}$	Annual	-0.11	-0.42 <sup>b</sup>	-0.23	0.01	0.02	-0.04	0.03	-0.04
	Rainy	-0.36 <sup>b</sup>	-0.44 <sup>b</sup>	-0.16	-0.12	-0.17	-0.16	-0.06	-0.05
	Dry	0.33 <sup>b</sup>	-0.01	0.17	-0.31 <sup>a</sup>	0.05	-0.33 <sup>b</sup>	-0.31 <sup>a</sup>	-0.31 <sup>a</sup>
R		<i>NINO</i>	<i>DMI</i>	$\overline{LAI}_{LP}$	$\overline{RH}_{LP}$	$\overline{Ta}_{LP}$	$\overline{Rn}_{LP}$	$\overline{SM}_{LP}$	$\overline{WS}_{LP}$
$E_{LP}$	Annual	0.00	0.18	0.75 <sup>b</sup>	-0.12	0.41 <sup>b</sup>	0.15	-0.16	0.04
	Rainy	-0.23	-0.02	0.63 <sup>b</sup>	0.34 <sup>b</sup>	0.27	0.04	0.13	0.13
	Dry	0.11	0.30 <sup>a</sup>	0.63 <sup>b</sup>	-0.18	0.44 <sup>b</sup>	0.33 <sup>b</sup>	-0.21	-0.07
R		<i>NINO</i>	<i>DMI</i>	$LAI_{LP}$	$RH_{LP}$	$Ta_{LP}$	$Rn_{LP}$	$SM_{LP}$	$WS_{LP}$
$ER_{LP}$	Annual	-0.15	-0.18	0.38 <sup>b</sup>	0.63 <sup>b</sup>	0.52 <sup>b</sup>	0.49 <sup>b</sup>	0.59 <sup>b</sup>	0.49 <sup>b</sup>
	Rainy	-0.35 <sup>b</sup>	-0.27	0.31 <sup>a</sup>	0.59 <sup>b</sup>	0.41 <sup>b</sup>	0.35 <sup>b</sup>	0.56 <sup>b</sup>	0.41 <sup>b</sup>
	Dry	0.28 <sup>a</sup>	0.05	0.49 <sup>b</sup>	0.58 <sup>b</sup>	0.53 <sup>b</sup>	0.46 <sup>b</sup>	0.43 <sup>b</sup>	0.27 <sup>a</sup>
R		<i>NINO</i>	<i>DMI</i>	$\overline{LAI}_{LP}$	$\overline{RH}_{LP}$	$\overline{Ta}_{LP}$	$\overline{Rn}_{LP}$	$\overline{SM}_{LP}$	$\overline{WS}_{LP}$
$ER_{LP}$	Annual	-0.15	-0.18	0.39 <sup>b</sup>	0.18	0.11	-0.29 <sup>a</sup>	0.07	0.03
	Rainy	-0.35 <sup>b</sup>	-0.27	0.31 <sup>a</sup>	0.51 <sup>b</sup>	-0.07	-0.39 <sup>b</sup>	0.20	0.14
	Dry	0.28 <sup>a</sup>	0.05	0.38 <sup>b</sup>	0.29 <sup>a</sup>	0.18	-0.19	-0.04	-0.47 <sup>b</sup>

<sup>a</sup>0.01 < *p* ≤ 0.05. <sup>b</sup>*p* ≤ 0.01.

The precipitationsheds for rainy season and dry season were identified by backward tracking the moisture source of 70% of the precipitation over the Loess Plateau (Figures 6e and 6f). If the area of precipitationshed increases, it could suggest that regional precipitation is more dependent on distant moisture sources. Conversely, a decrease in precipitationshed area indicates that the moisture sources are more concentrated, and the region may be more sensitive to local environmental changes. The change in precipitationshed area may, in turn, indicate instability in regional climate, ecosystems, and atmospheric circulation. In general, the area of precipitationshed for 2000–2019 was smaller than that for 1982–1999 (Figure 6d), suggesting a weaker contribution from south and west. During the rainy season, the precipitationshed contrasted by about 4.3% of the simulated domain, showing a decline of the contribution from Indian Ocean, Eastern European, and Siberian Plain (Figure 6e). While during the dry season, the precipitationshed contrasted by about 1.8%, shrinking mainly from southward, suggesting a weaker impact from the ocean (Figure 6f).

### 3.4. Impacts of Vegetation Restoration on Precipitation Over the Loess Plateau

Vegetation modifies the land surface properties, and mediates the exchange between the land and the atmosphere. In this study, we adopted a hydrologically weighting method to quantify the hydrologically effect of the environmental factors on precipitation. The correlation efficient between  $ER_{LP}$  and hydrologically weighted values of the environmental factors were much more significant than that of simply regional averaged values (Table 1), indicating that hydrological weighted variables can better reflect their connection with atmosphere moisture recycling. As shown in Table 1, local evaporation is significantly correlated with  $\overline{LAI}_{LP}$  in both the rainy season and dry season, and locally recycled moisture also shows positive correlation with the  $LAI_{LP}$ , implying that vegetation had a prompt impact on local evaporation and moisture recycling. However, the correlation between precipitation and regional effective LAI was negative in the rainy season, while was positive in the dry season, suggesting a seasonal discrepancy in the relationship between regional vegetation and precipitation over the Loess Plateau. According to the analyses of the Stepwise Selection Method, vegetation consistently played an essential role in evaporation on the Loess Plateau, and was important for locally recycled moisture in the dry season, as well as the precipitation in the rainy season (Figure 7). Meanwhile, the variability of vegetation had a moderate impact on the variations of evaporation throughout the year, precipitation in the rainy season, and locally recycled moisture in the rainy season. Detailed results can be found in Table S2 in Supporting Information S1.

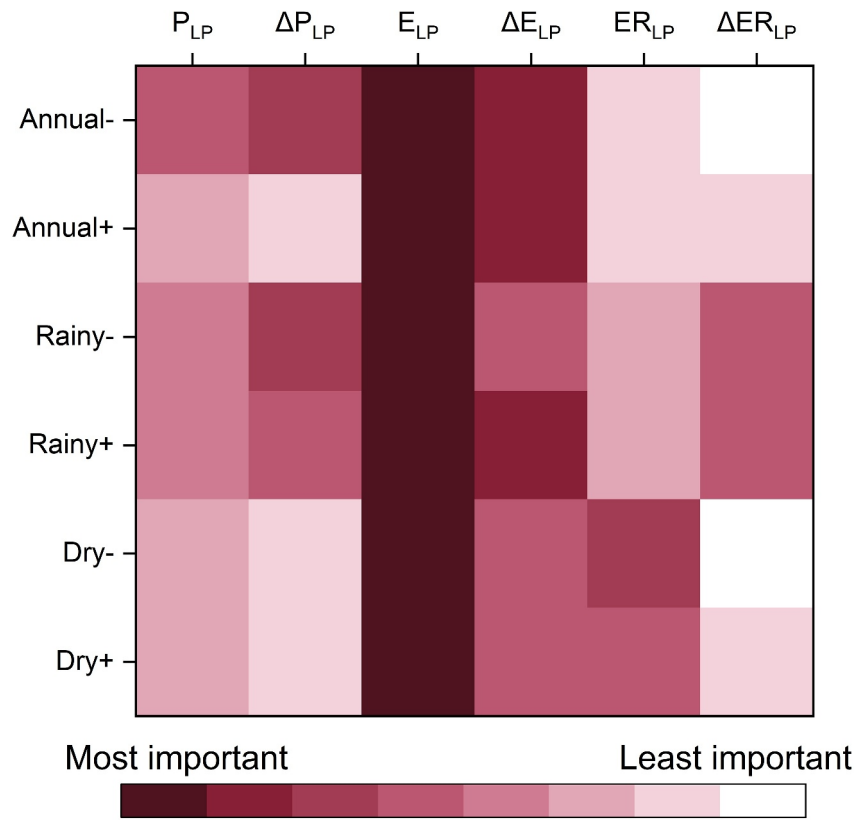


**Figure 7.** The importance of LAI on water cycling in Loess Plateau, ranked by the Stepwise Selection method. The plus sign (“+”) denotes the forward selection and the minus sign (“-”) denotes backward selection.  $\Delta P_{LP}$ ,  $\Delta E_{LP}$ , and  $\Delta ER_{LP}$  represent the variance of the regional-averaged  $P$ ,  $E$  and  $ER$ , which were calculated as the differences between the values of successive years.

The effect of the revegetation on precipitation over the Loess Plateau was quantified by multiplying the sensitivity of locally recycled moisture ( $ER_{LP}$ ) to local effective LAI ( $LAI_{LP}$ ) by the trend of local effective LAI (Equation 15). Here we present the range of values obtained using three different LAI products, to account for observational uncertainties. After 2000, vegetation increased the  $E_{LP}$  by  $5.22 \pm 0.36$ ,  $7.14 \pm 0.46$  and  $6.14 \pm 0.49$   $\text{mm yr}^{-1}$  based on LAI from GLASS, GIMMS and GLOBMAP respectively, leading to a change of the  $ER_{LP}$  by  $0.06 \pm 0.10$ ,  $0.04 \pm 0.13$  and  $0.10 \pm 0.10$   $\text{mm yr}^{-1}$  (Figures 8b and 8c). As the local effective LAI ( $LAI_{LP}$ ) had increasing trends during both seasons, it exerted an effect of about 0.11  $\text{mm yr}^{-1}$  on local precipitation in the rainy season and about 0.11  $\text{mm yr}^{-1}$  in the dry season (Figure 9a; Figure S4 in Supporting Information S1). Meanwhile, the regional greening has resulted in a change of about 0.83  $\text{mm yr}^{-1}$  (GLASS:  $0.29 \pm 0.10$   $\text{mm yr}^{-1}$ ; GIMMS:  $0.52 \pm 0.17$   $\text{mm yr}^{-1}$ ; GLOBMAP:  $1.68 \pm 0.43$   $\text{mm yr}^{-1}$ ) on precipitation over the Loess Plateau, with contributions of about 0.07 and 0.76  $\text{mm yr}^{-1}$  in the rainy season and dry season, respectively.

The change of  $E_r$  in each grid cell can be considered as the result of the integrated effect of  $E$  and  $\epsilon$ , of which  $\epsilon$  can identify the strength of hydrological land surface-atmosphere coupling (Goessling & Reick, 2011). To explore the potential reasons for the changes in  $P$  over the Loess Plateau, we selected grid cells where the changes in  $E_r$ ,  $E$ , and  $\epsilon$  were relatively pronounced. As shown in Figure 10, about 30.3% of area experienced an increasing trend in  $E_r$ , while about 42.8% of area experienced a decreasing trend. The increase of  $E_r$  is primarily attributed to the simultaneous increases in  $E$  and  $\epsilon$ , accounting for 12.1% of the area. In contrast, with simultaneous decreases in both  $E$  and  $\epsilon$ ,  $E_r$  experienced a definite decrease, accounting for about 21.8% of the area. When  $E$  and  $\epsilon$  change in opposite directions, the change in  $E_r$  tends to align more with  $\epsilon$ . Approximately 18.6% of the areas where  $E_r$  decreased experienced an increase in  $E$  and a decrease in  $\epsilon$ , and 9.9% of the areas where  $E_r$  increased experienced a decrease in  $E$  and an increase in  $\epsilon$ . When focusing on the region within the precipitationshed, the increase in  $E_r$  generally associated with a rise in  $E$ , while a decrease in  $E_r$  is often accompanied by a decline in  $\epsilon$  (Figure 10).

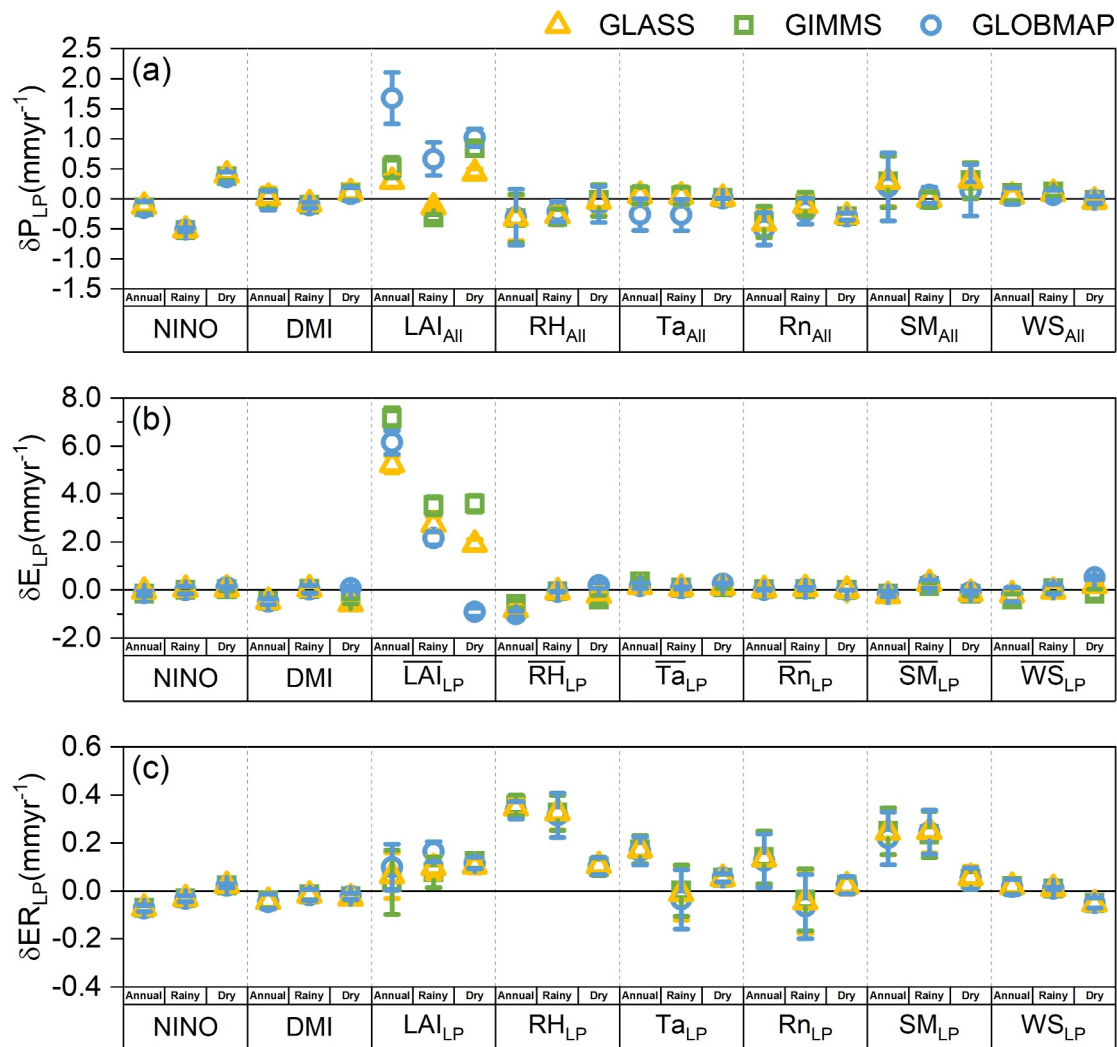


**Figure 8.** The attribution of environmental factors to the change of  $P_{LP}$ ,  $E_{LP}$ , and  $ER_{LP}$ .

This indicates that precipitation changes in the Loess Plateau result from the interplay of two forces: an increase in evaporation within the precipitationshed and a reduction in  $\varepsilon$ , which can be roughly considered a proxy of local thermally and dynamically effects and large-scale atmospheric circulations (Goessling & Reick, 2011).

## 4. Discussion

### 4.1. Atmosphere Moisture Recycling Over Loess Plateau

In this study, we first investigated the changes in the atmospheric water cycle over the Loess Plateau using the modified WAM-2layers model (Xiao & Cui, 2021). Our results show that most of China -eastern Central Asia are the major sources of moisture uptake over the Loess Plateau. These results are consistent with the findings of Hu et al. (2018), who used the Lagrangian flexible particle dispersion model (FLEXPART) and the areal source-receptor attribution method. Local evaporation and atmospheric moisture are strongly associated with precipitation. Our results indicate that local evaporation contributed about 7.7% of the precipitation over the Loess Plateau, and the proportion increased from 6.9% to 8.3% after 2000 (Figure 4e). These findings are of the same order of magnitude as a similar study using WRF-WVT/WRF-DPRM model and suggest that the precipitation recycling ratio increased from 9.06% to 10.18% after the Grain for Green Project (S. Chen, Xiong, et al., 2023; W. Chen, Xiong, et al., 2023; Liu et al., 2023; Tian et al., 2022). In light of the substantial spatial overlap between the Loess Plateau and the Yellow River Basin, we included studies conducted within the Yellow River Basin as

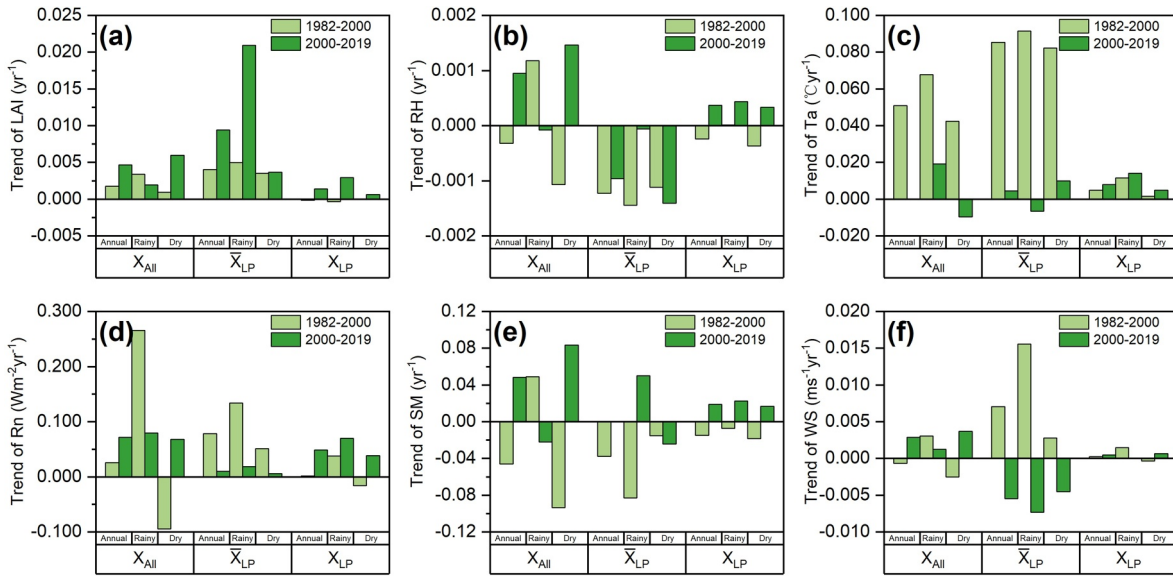


**Figure 9.** The trends of the regional effective values ( $X_{All}$ ), regional averaged values ( $\bar{X}_{LP}$ ) and local effective values ( $X_{LP}$ ) for different variables.

references. Using a Lagrangian atmospheric moisture tracking model (UTrack), Wang, Liu, et al. (2023) suggested evaporation from the Yellow River Basin contributed 7% of local precipitation from 1980 to 2018, which is in agreement with our finding.

In order to evaluate the uncertainty caused by input data, especially the precipitation and evaporation,  $P$  from MSWEP and ERA5, and  $E$  from MERRA2 and ERA5, were used to force the WAM-2layers model in four different input configurations. Although significant differences were found in these products over the Loess Plateau, the results of the four experiments are relatively similar (Figures S2–S3, and S8–S9 in Supporting Information S1). However, the moisture tracking results were more sensitive to the evaporation products and showed more significant differences in local contributions. Additionally, precipitation sheds driven by MERRA2  $E$  covered larger areas than those driven by ERA5.

To further assess the uncertainty derived from the model, we compared the moisture tracking results from the WAM-2layers model with the UTrack data set, which is a global data set on moisture recycling from evaporation to precipitation with a climatological mean from 2008 to 2017 (Tuinenburg et al., 2020). We conducted an additional set of experiments from 2008 to 2017 using WAM-2layers driven by the same ERA5 reanalysis. As shown Figure S10 in Supporting Information S1, although moisture is recycled from the west and south through

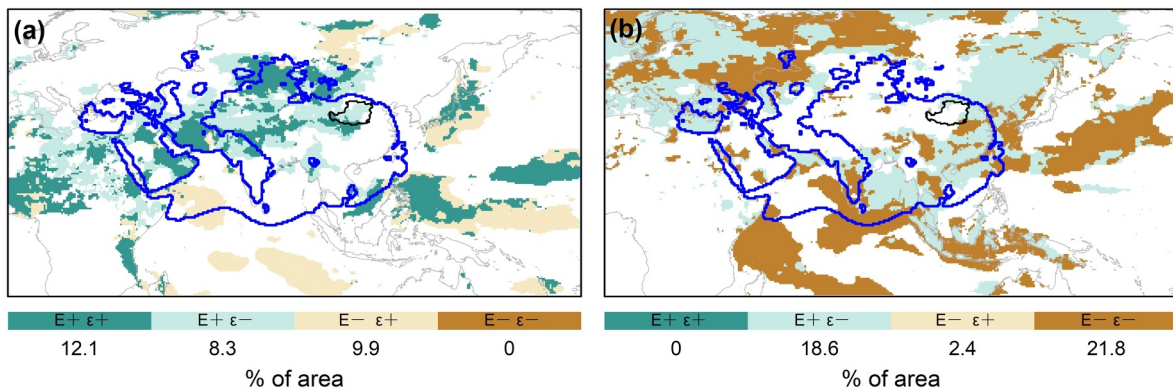


**Figure 10.** The change direction of evaporation ( $E$ ) and evaporation recycling ratio ( $\epsilon$ ) when recycled moisture ( $ER$ ) is (a) increasing and (b) decreasing. The blue line denotes the boundary of the precipitation shed. Dark green represents an increase in both  $E$  and  $\epsilon$ ; light green represents an increase in  $E$  and a decrease in  $\epsilon$ ; light brown represents a decrease in  $E$  and an increase in  $\epsilon$ ; dark brown represents a decrease in both  $E$  and  $\epsilon$ .

the westerlies and the East Asian Monsoon in both models, the pattern is significantly different over the Tibetan Plateau. The recycled moisture using WAM-2layers tends to cover a wider area, exerting strong influences over long distances. In contrast, moisture using UTrack tends to be recycled over shorter distances. Additionally, the concentration intensity using UTrack is much higher than that of WAM-2layers.

#### 4.2. The Net Impact of the Revegetation Over the Loess Plateau on Precipitation

Following the launch of the Grain for Green Project, the Loess Plateau has exhibited a noteworthy greening trend (Figure 3), accompanied by a local drying trend, concurrently prompting concerns about water sustainability. Intuitively, vegetation growth will promote local precipitation by increasing local evaporation, thereby leading to an increase in precipitable moisture. Indeed, that is the case, as the greening caused an increase of 5.22–7.14 mm yr<sup>-1</sup> in evaporation within the Loess Plateau. Consequently, precipitation recycling from local evaporation has also increased. As shown in Table 1, the changes in local effective LAI (LAI<sub>LP</sub>) and locally recycled moisture ( $ER_{LP}$ ) exhibit a significant positive correlation ( $R = 0.38$ ), which is more pronounced in the dry season than the rainy season. Spatially, we observed that regions where  $E_r$  show notable growth trend coincide with significant increase in LAI by comparing Figure 3 with Figures 5j and 5k. These findings align with the results drawn from the attribution analysis. The vegetation is sensitive to locally recycled moisture, and the rise in LAI<sub>LP</sub> after 2000 accounts for the change of precipitation by about 0.07 mm yr<sup>-1</sup> (GLASS: 0.06 ± 0.10 mm yr<sup>-1</sup>; GIMMS: 0.04 ± 0.13 mm yr<sup>-1</sup>; GLOBMAP: 0.10 ± 0.10 mm yr<sup>-1</sup>). Additionally, the attribution of local vegetation to precipitation is similar but with higher uncertainty in the rainy season (GLASS: 0.10 ± 0.05 mm yr<sup>-1</sup>; GIMMS: 0.08 ± 0.06 mm yr<sup>-1</sup>; GLOBMAP: 0.16 ± 0.04 mm yr<sup>-1</sup>) compared to the dry season (GLASS: 0.10 ± 0.03 mm yr<sup>-1</sup>; GIMMS: 0.12 ± 0.03 mm yr<sup>-1</sup>; GLOBMAP: 0.12 ± 0.02 mm yr<sup>-1</sup>) (Figure 8). Studies using WRF-DPRM model suggest that revegetation project has elevated the internal branch of the atmosphere water cycle by 8.23 mm for the whole year and 5.03 mm during the rainy season until 2015 (S. Chen, Xiong, et al., 2023; W. Chen, Xiong, et al., 2023; Tian et al., 2022). Their findings are higher than the result of our study, which is -1.95 to 3.89 mm for the whole year and 0.27–4.12 mm during the rainy season. The differences in our findings may stem from the fact that their conclusions are drawn from model experience, whereas ours are based on observational evidence. Notably, when analyzing the uncertainty arising from input data sets, we found that the results consistently show that the revegetation over the Loess Plateau has a positive effect on local precipitation through recycled moisture (Figure S11 in Supporting Information S1).

Furthermore, the enhanced evaporation caused by revegetation is projected to precipitate not only within the Loess Plateau but also outside the region. The evaporation flow to the downwind area out of the Loess Plateau rises at the rate of 4.5 mm yr<sup>-1</sup>, accounting for 87% of the total evaporation growth trend (Figure 4d). The increase of moisture transfer outside the region in the dry season is greater than in the rainy season (Figure S7 in Supporting Information S1). Higher exports can be explained by changes in the wind pattern transporting moisture or effect of positive land use change to the surrounding regions.

#### 4.3. The Causes of the Change of Precipitation Over the Loess Plateau

This study further scrutinized the causes for the increased precipitation over the Loess Plateau under simultaneous global warming and vegetation restoration. By adopting the hydrologically weighting method, we quantify the effect of the environmental factors both within the Loess Plateau and regionally (region here including the Loess Plateau). After 2000, the LAI<sub>All</sub>, RH<sub>All</sub>, Rn<sub>All</sub>, SM<sub>All</sub> and WS<sub>All</sub> all showed increasing trends on an annual scale (Figure 9). The Ta<sub>All</sub> has an increasing trend in the rainy season, while had a decreasing trend in the dry season. The regional averaged RH and SM both exhibit decreasing trends, which is consistent with previous studies (Zhang et al., 2018). However, the RH<sub>All</sub> and SM<sub>All</sub> had increasing trends after 2000, indicating that although the Loess Plateau is experiencing a drying trend, the effective influence of regional atmospheric moisture and soil moisture on the Loess Plateau is wetting.

Overall, regional greening is the main reason for the increase in precipitation on the Loess Plateau. Cui et al. (2022) found a globally averaged increase of 11.0 mm of precipitation can be attributed to changes in weighted effective LAI during 2001–2018. In this study, the change in Loess Plateau precipitation caused by regional greening is approximately 0.83 mm yr<sup>-1</sup> (Figure 8). Generally, regional greening has increased the precipitation on the Loess Plateau, with the range of 0.19–2.10 mm yr<sup>-1</sup> for the whole year and 0.36–1.16 mm yr<sup>-1</sup> for the dry seasons. However, the conclusion regarding whether regional effective LAI had a



positive or negative impact on rainy season precipitation in our study depends largely on the choice of LAI products. Among them, results drawn from GLOBMAP show an enhancement effect, reaching  $0.66 \pm 0.28 \text{ mm yr}^{-1}$ , while those from GLASS and GIMMS are  $-0.14 \pm 0.03$  and  $-0.32 \pm 0.05 \text{ mm yr}^{-1}$ , respectively. We also analyzed the uncertainty arising from the precipitation and evaporation data sets. Despite numerical differences, the effect of vegetation on precipitation, whether increasing or decreasing, is not affected by the choice of input data for precipitation or evaporation (Figure S12 in Supporting Information S1). Moreover, revegetation over the Loess Plateau has a high probability of increasing effect on local precipitation. In the rainy season when vegetation grows vigorously,  $LAI_{LP}$  promoted the rise of Loess Plateau precipitation by about  $0.11 \text{ mm yr}^{-1}$ , while that in the dry season was also about  $0.11 \text{ mm yr}^{-1}$ .

Meanwhile, the attribution of regional effective  $T_a$  was about  $-0.05 \text{ mm yr}^{-1}$  (GLASS:  $0.05 \pm 0.15 \text{ mm yr}^{-1}$ ; GIMMS:  $0.06 \pm 0.15 \text{ mm yr}^{-1}$ ; GLOBMAP:  $-0.26 \pm 0.26 \text{ mm yr}^{-1}$ ), indicating a buffering effect on the precipitation. As for  $T_{a,LP}$ , it showed an almost negligible negative impact in the rainy season, while showed a positive impact in the dry season. In fact, apart from  $LAI_{All}$ ,  $SM_{All}$  and  $WS_{All}$ , all other regional effective variables showed a decreasing effect on precipitation. When separating the contribution of the Loess Plateau, actually all of the terrestrial environmental factors increased the local precipitation (Figure 8). While the majority of the environmental factors show consistent positive or negative results due to variations in input data for precipitation and evaporation, there are cases where both positive and negative effects coexist (Figure S12 in Supporting Information S1). In this study, we favor the combination of MSWEP precipitation and MERRA evaporation as the more reliable choice.

Climate changes can also lead to changes in horizontal moisture transport (Lavers et al., 2015). It has been well demonstrated that large-scale atmospheric circulation patterns are responsible for the spatial and temporal variability of rainfall (Ren et al., 2022; Tan et al., 2014). Wang et al. (2019) identified that rainy season precipitation over the Loess Plateau predominantly originates from the Indian and Pacific oceans, rendering it vulnerable to large-scale climate variability, such as sea surface temperature anomalies over the eastern Pacific. Two climate variability indices are adopted to represent the change of sea surface temperature in this study. NINO is used to represent the strength of ENSO, which is regarded as the changes of sea surface temperature in the eastern Pacific Ocean. DMI is adopted to assess the strength of the IOD, which is characterized by anomalies in sea surface temperatures between the western and eastern parts of the Indian Ocean. As illustrated in Table 1, the influence of ENSO and IOD on evaporation over the Loess Plateau is not significant, due to its inland location. ENSO exhibits significant negative correlations with precipitation and locally recycled moisture during the rainy season, while shows significant positive correlations during the dry season. In the rainy season, IOD manifests a significant negative impact on locally moisture recycling (Figure 8). Moreover, we quantified the impact of ENSO and IOD on the precipitation over the Loess Plateau. In the rainy season, ENSO and IOD had a negative effect, with  $-0.52$  and  $-0.10 \text{ mm yr}^{-1}$ , respectively. While in the dry season, ENSO contributes to an increasing trend by about  $0.38 \text{ mm yr}^{-1}$ , and IOD has a positive effect of about  $0.09 \text{ mm yr}^{-1}$ . These results are consistent with the mechanisms underlying ENSO and IOD. In El Niño years, a weakened monsoon influenced by an anomalous western Pacific high, reduces precipitation in the rainy season. However, during the dry season, the extended subtropical high-pressure system increases moisture transport, leading to increased precipitation. In contrast, La Niña intensifies the monsoon, increasing rainy season moisture transport but reducing it in the dry season. Meanwhile, the stronger the IOD strength, the weaker the convective activity in the eastern Indian Ocean, which suppresses the East Asian monsoon system during the rainy season and reduces moisture transport from the Indian Ocean. At the same time, increased convective activity in the western Indian Ocean influences the westerlies, leading to increased precipitation during the dry season. In contrast, when the IOD is negative, convective activity increases in the eastern Indian Ocean and decreases in the western Indian Ocean, leading to increased precipitation in the rainy season, and decreased precipitation in the dry season.

#### 4.4. Water Budget Changes Over the Loess Plateau

As the increase in evaporation outweighs the increase in precipitation, we examined the changes in the water balance over the Loess Plateau from 2000 to 2019 (Figure S13 in Supporting Information S1). The decrease in the water budget suggests that vegetation restoration has led to an increase water consumption across the region, while the increase in precipitation has not been sufficient to compensate for the loss. Given the observed upward trend in runoff, the water required for evaporation was most likely supplied by soil moisture. Previous studies, based on in situ observations, meta-analyses, and remote sensing data sets, have indicated that soil moisture

decreased after land use conversion, particularly in deeper soil layers (Feng et al., 2016; Jia et al., 2017; Li et al., 2021; Su & Shanguan, 2018). As illustrated in Figure S13b in Supporting Information S1, soil moisture over the Loess Plateau has indeed exhibited a declining trend from 2000 to 2019, with a similar decreasing trend observed in monthly Terrestrial Water Storage from 2002 to 2019.

The effect of the revegetation on the water budget of the Loess Plateau in this study can be considered as a combined effect on local recycled moisture and evaporation. As shown in Figure S14 in Supporting Information S1, the growth of local vegetation has led to a decreasing trend in the water budget, accounting for about  $-7.11-5.16 \text{ mm yr}^{-1}$ . The effect of the vegetation during the rainy season is relatively constant, reducing the local water budget by about  $-2.69 \text{ mm yr}^{-1}$ . However, during the dry season, the effect varies depending on the product selected.

#### 4.5. Limitations

While the extensive sensitivity analyses and the reasonable agreement between our estimates and those reported in previous research corroborate the overall methodological framework proposed here, a series of potential limitations should be carefully considered. First, the moisture tracking results rely heavily on the accuracy of input data sets and the fitness of the model (van der Ent et al., 2013; Zhang et al., 2023). Comparing various precipitation and evaporation products that drove the model, we found significant disparities in the reanalysis products over the Loess Plateau (Figures S2–S3 in Supporting Information S1). Despite selecting the data most suitable for this study, considerable uncertainties persist (Figures S8–S10 in Supporting Information S1). Also, attribution analysis is a further potential source of uncertainty. Though we employed a range of value in sensitivity calculation rather than a singular value, it just explained approximately 30%, 60% and 60% of the variance for precipitation, evaporation and locally recycled moisture respectively. Second, we investigated the revegetation or greening, rather than the Grain for Green Project in this study. In other words, we did not make a distinction between greening caused by natural vegetation dynamics and anthropogenic alterations on the Loess Plateau. Hence, we caution against directly linking our results to the impact of project. Last, given that about 91% of moisture that evaporated from the Loess Plateau will flow out of the plateau, the impact of the revegetation may thus strongly influence the precipitation downwind. The ultimate fate of this moisture remains to be investigated. The spatial patterns and variations of the Loess Plateau evaporation, especially under the global warming and greening background, are of significant scientific interest and warrant close investigation.

#### 5. Conclusion

The Loess Plateau in China has experienced a significant greening trend due to vegetation restoration in recent decades. However, it remains unclear how the atmospheric branch of the hydrological cycle responds to greening. In this study, moisture sources for precipitation over the Loess Plateau during 1982–2019 were identified and evaluated using the modified WAM-2layers model and the conceptual framework of precipitationshed. We then introduce a hydrologically weighting method and the multiple linear regression model to quantify the effective influence of different environmental factors on precipitation. We found that local precipitation has increased on average by  $0.16 \text{ mm yr}^{-1}$  and evaporation has increased by  $5.17 \text{ mm yr}^{-1}$  in the period 2000–2019 after the initiation of the revegetation project. After eliminating the influence of other factors, regional greening including the Loess Plateau is responsible for precipitation changes of  $0.29 \pm 0.10$ ,  $0.52 \pm 0.17$  mm, and  $1.68 \pm 0.43 \text{ mm yr}^{-1}$  based on LAI from GLASS, GIMMS and GLOBMAP respectively, while local revegetation contributes for  $0.06 \pm 0.10$ ,  $0.04 \pm 0.13$  and  $0.10 \pm 0.10 \text{ mm yr}^{-1}$  respectively. The local vegetation contribution results from both increased local evaporation and enhanced local recycling, with the local contribution ratio increasing from 6.9% in 1982–1999 to 8.3% in 2000–2019. Thus, our study highlights that local revegetation has had a positive effect on local precipitation, and along with changes in moisture circulation, is a major contributor to the observed increase in precipitation over the Loess Plateau. Our study provides valuable information for landscape management and policy making in terms of climate mitigation and adaptation.

#### Conflict of Interest

The authors declare no conflicts of interest relevant to this study.

## Data Availability Statement

The ERA5 reanalysis products were obtained from the ECMWF via <https://cds.climate.copernicus.eu/>. The MERRA-2 reanalysis products were obtained from the NASA Goddard Earth Sciences Data and Information Services Center via <https://doi.org/10.5067/7MCPBJ41Y0K6> and <https://doi.org/10.5067/0JRLVL8YV2Y4> (GMAO, 2015a; GMAO, 2015b). The MSWEP data was obtained via <https://www.gloh2o.org/mswep/>. The GLASS LAI data set was obtained via [https://doi.org/10.12041/geodata.GLASS\\_LAI\\_modis\(0.05D\).ver1.db](https://doi.org/10.12041/geodata.GLASS_LAI_modis(0.05D).ver1.db) (Liang, 2021), the GIMMS LAI data set was downloaded from Zenodo (Cao et al., 2023), and the GLOBMAP LAI data was downloaded from Zenodo (Liu et al., 2021). The Python code for the modified WAM-2layers model was downloaded from Zenodo (Xmingzh, 2021). The modeled and resulting data that support this study and the scripts used to analyze are openly available online in a Zenodo repository (Cao et al., 2024).

## Acknowledgments

This work was jointly supported by the National Natural Science Foundation of China (U2240218, 52479010, 51979071) and China Scholarship Council (CSC) Grant (202206710089). J.W. is supported by the National Natural Science Foundation of China (42307117), the Fundamental Research Funds for the Central Universities (B230201039), China Postdoctoral Science Foundation (2023M740984). L.W.-E. is supported by funding from Formas (2019-01220, 2022-02089, 2023-0310 and 2023-00321), the IKEA foundation, the Marianne and Marcus Wallenberg Foundation, and the Marcus and Amalia Wallenberg Foundation, Horizon Europe (101081661), and the European Research Council (ERC) (ERC-2016-ADG-743080). G.F. was supported by the Horizon Europe Project ECO2ADAPT (Grant Agreement n. 101059498). IF was funded by the European Research Council (Project Earth Resilience in the Anthropocene, ERC-2016-ADG 743080) and MISTRA project FAIRTRANS.

## References

- Achugbu, I. C., Laux, P., Olufayo, A. A., Balogun, I. A., Dudhia, J., Arnault, J., et al. (2022). The impacts of land use and land cover change on biophysical processes in West Africa using a regional climate model experimental approach. *International Journal of Climatology*, 43(4), 1731–1755. <https://doi.org/10.1002/joc.7943>
- Albaugh, J. M., Dye, P. J., & King, J. S. (2013). Eucalyptus and water use in South Africa. *International Journal of Financial Research*, 2013, 1–11. <https://doi.org/10.1155/2013/852540>
- Baudena, M., Tuinenburg, O. A., Ferdinand, P. A., & Staal, A. (2021). Effects of land-use change in the Amazon on precipitation are likely underestimated. *Global Change Biology*, 27(21), 5580–5587. <https://doi.org/10.1111/gcb.15810>
- Beaudoin, H., & Rodell, M., & NASA/GSFC/HSL. (2020). *GLDAS NOAA land surface model L4 monthly 0.25 x 0.25 degree V2.1*. Goddard Earth Sciences Data and Information Services Center (GES DISC). <https://doi.org/10.5067/SXAVCZFAQLNO>
- Beck, H. E., van Dijk, A. I. J. M., Levizzani, V., Schellekens, J., Miralles, D. G., Martens, B., & de Roo, A. (2017). Mswep: 3-hourly 0.25° global gridded precipitation (1979–2015) by merging gauge, satellite, and reanalysis data. *Hydrology and Earth System Sciences*, 21(1), 589–615. <https://doi.org/10.5194/hess-21-589-2017>
- Bonan, G. B., Pollard, D., & Thompson, S. L. (1992). Effects of boreal forest vegetation on global climate. *Nature*, 359(6397), 716–718. <https://doi.org/10.1038/359716a0>
- Branch, O., & Wulfmeyer, V. (2019). Deliberate enhancement of rainfall using desert plantations. *Proceedings of the National Academy of Sciences*, 116(38), 18841–18847. <https://doi.org/10.1073/pnas.1904754116>
- Brubaker, K. L., Entekhabi, D., & Eagleson, P. S. (1993). Estimation of continental precipitation recycling. *Journal of Climate*, 6(6), 1077–1089. [https://doi.org/10.1175/1520-0442\(1993\)006<1077:EOCPR>2.0.CO;2](https://doi.org/10.1175/1520-0442(1993)006<1077:EOCPR>2.0.CO;2)
- Cao, M., Wang, W., Wei, J., Forzieri, G., Fetzer, I., & Wang-Erlandsson, L. (2024). Data and code for paper revegetation impacts on moisture recycling and precipitation trends in the Chinese Loess Plateau [Dataset]. *Zenodo*. <https://doi.org/10.5281/zenodo.13938853>
- Cao, S., Li, M., Zhu, Z., Wang, Z., Zha, J., Zhao, W., et al. (2023). Spatiotemporally consistent global dataset of the GIMMS leaf area index (GIMMS LAI4g) from 1982 to 2020 (V1.2) (V1.2) [Dataset]. *Zenodo*. <https://doi.org/10.5281/zenodo.8281930>
- Chambers, J. M., & Hastie, T. J. (1992). Generalized linear models. In *Chapter 6 of statistical models in S*. Wadsworth and Brooks/Cole.
- Chen, M., Shi, W., Xie, P., Silva, V. B. S., Kousky, V. E., Wayne Higgins, R., & Janowiak, J. E. (2008). Assessing objective techniques for gauge-based analyses of global daily precipitation. *Journal of Geophysical Research*, 113(D4). <https://doi.org/10.1029/2007JD009132>
- Chen, S., Tian, L., Zhang, B., Zhang, G., Zhang, F., Yang, K., et al. (2023). Quantifying the impact of large-scale afforestation on the atmospheric water cycle during rainy season over the Chinese Loess Plateau. *Journal of Hydrology*, 619, 129326. <https://doi.org/10.1016/j.jhydrol.2023.129326>
- Chen, W., Xiong, Y., Zhong, M., Yang, Z., Shum, C. K., Li, W., et al. (2023). Twenty-year spatiotemporal variations of TWS over mainland China observed by GRACE and GRACE follow-on satellites. *Atmosphere*, 14(12), 1717. <https://doi.org/10.3390/atmos14121717>
- Chen, Z., Wang, W., Cescatti, A., & Forzieri, G. (2022). Climate-driven vegetation greening further reduces water availability in drylands. *Global Change Biology*, 29(6), 1628–1647. <https://doi.org/10.1111/gcb.16561>
- Cui, J., Lian, X., Huntingford, C., Gimeno, L., Wang, T., Ding, J., et al. (2022). Global water availability boosted by vegetation-driven changes in atmospheric moisture transport. *Nature Geoscience*, 15(12), 982–988. <https://doi.org/10.1038/s41561-022-01061-7>
- de Noblet-Ducoudré, N., Boisier, J.-P., Pitman, A., Bonan, G. B., Brovkin, V., Cruz, F., et al. (2012). Determining robust impacts of land-use-induced land cover changes on surface climate over North America and Eurasia: Results from the first set of LUCID experiments. *Journal of Climate*, 25(9), 3261–3281. <https://doi.org/10.1175/jcli-d-11-00338.1>
- Doelman, J. C., Stehfest, E., van Vuuren, D. P., Tabeau, A., Hof, A. F., Braakhekke, M. C., et al. (2019). Afforestation for climate change mitigation: Potentials, risks and trade-offs. *Global Change Biology*, 26(3), 1576–1591. <https://doi.org/10.1111/gcb.14887>
- Farley, K. A., Jobbágy, E. G., & Jackson, R. B. (2005). Effects of afforestation on water yield: A global synthesis with implications for policy. *Global Change Biology*, 11(10), 1565–1576. <https://doi.org/10.1111/j.1365-2486.2005.01011.x>
- Feng, X., Fu, B., Piao, S., Wang, S., Ciais, P., Zeng, Z., et al. (2016). Revegetation in China's Loess Plateau is approaching sustainable water resource limits. *Nature Climate Change*, 6(11), 1019–1022. <https://doi.org/10.1038/nclimate3092>
- Forzieri, G., Alkama, R., Miralles, D. G., & Cescatti, A. (2017). Satellites reveal contrasting responses of regional climate to the widespread greening of Earth. *Science*, 356(6343), 1180–1184. <https://doi.org/10.1126/science.aal1727>
- Forzieri, G., Duveiller, G., Georgievski, G., Li, W., Robertson, E., Kautz, M., et al. (2018). Evaluating the interplay between biophysical processes and leaf area changes in land surface models. *Journal of Advances in Modeling Earth Systems*, 10(5), 1102–1126. <https://doi.org/10.1002/2018ms001284>
- Forzieri, G., Miralles, D. G., Ciais, P., Alkama, R., Ryu, Y., Duveiller, G., et al. (2020). Increased control of vegetation on global terrestrial energy fluxes. *Nature Climate Change*, 10(4), 356–362. <https://doi.org/10.1038/s41558-020-0717-0>
- Friedl, M., & Sulla-Menashe, D. (2022). MODIS/Terra+Aqua land cover type yearly L3 global 0.05Deg CMG V061 [Dataset]. *NASA EOSDIS Land Processes Distributed Active Archive Center*. <https://doi.org/10.5067/MODIS/MCD12C1.061>
- García-Carreras, L., & Parker, D. J. (2011). How does local tropical deforestation affect rainfall? *Geophysical Research Letters*, 38(19). <https://doi.org/10.1029/2011gl049099>

- Ge, J., Pitman, A. J., Guo, W., Zan, B., & Fu, C. (2020). Impact of revegetation of the Loess Plateau of China on the regional growing season water balance. *Hydrology and Earth System Sciences*, 24(2), 515–533. <https://doi.org/10.5194/hess-24-515-2020>
- Global Modeling and Assimilation Office (GMAO). (2015a). MERRA-2 tavg1\_2d\_flux\_Nx: 2d,1-Hourly,Time-Averaged,Single-Level,Assimilation,Surface flux diagnostics V5.12.4 [Dataset]. *Goddard Earth Sciences Data and Information Services Center (GES DISC)*. <https://doi.org/10.5067/7MCPBJ41YOK6>
- Global Modeling and Assimilation Office (GMAO). (2015b). MERRA-2 tavgM\_2d\_flux\_Nx: 2d,Monthly mean,Time-Averaged,Single-Level,Assimilation,Surface flux diagnostics V5.12.4 [Dataset]. *Goddard Earth Sciences Data and Information Services Center (GES DISC)*. <https://doi.org/10.5067/0JRLVL8YV2Y4>
- Goessling, H. F., & Reick, C. H. (2011). What do moisture recycling estimates tell us? Exploring the extreme case of non-evaporating continents. *Hydrology and Earth System Sciences*, 15(10), 3217–3235. <https://doi.org/10.5194/hess-15-3217-2011>
- Gonsamo, A., Ciais, P., Miralles, D. G., Sitch, S., Dorigo, W., Lombardozzi, D., et al. (2021). Greening drylands despite warming consistent with carbon dioxide fertilization effect. *Global Change Biology*, 27(14), 3336–3349. <https://doi.org/10.1111/gcb.15658>
- Harris, I., Osborn, T. J., Jones, P., & Lister, D. (2020). Version 4 of the CRU TS monthly high-resolution gridded multivariate climate dataset. *Scientific Data*, 7(1), 109. <https://doi.org/10.1038/s41597-020-0453-3>
- Hersbach, H., Bell, B., Berrisford, P., Hirahara, S., Horányi, A., Muñoz-Sabater, J., et al. (2020). The ERA5 global reanalysis. *Quarterly Journal of the Royal Meteorological Society*, 146(730), 1999–2049. <https://doi.org/10.1002/qj.3803>
- Hoek van Dijke, A. J., Herold, M., Mallick, K., Benedict, I., Machwitz, M., Schlerf, M., et al. (2022). Shifts in regional water availability due to global tree restoration. *Nature Geoscience*, 15(5), 363–368. <https://doi.org/10.1038/s41561-022-00935-0>
- Hu, Q., Jiang, D., Lang, X., & Xu, B. (2018). Moisture sources of the Chinese Loess Plateau during 1979–2009. *Palaeogeography, Palaeoclimatology, Palaeoecology*, 509, 156–163. <https://doi.org/10.1016/j.palaeo.2016.12.030>
- Jia, X., Shao, M. a., Zhu, Y., & Luo, Y. (2017). Soil moisture decline due to afforestation across the Loess Plateau, China. *Journal of Hydrology*, 546, 113–122. <https://doi.org/10.1016/j.jhydrol.2017.01.011>
- Jiang, C., & Ryu, Y. (2016). Multi-scale evaluation of global gross primary productivity and evapotranspiration products derived from Breathing Earth System Simulator (BESS). *Remote Sensing of Environment*, 186, 528–547. <https://doi.org/10.1016/j.rse.2016.08.030>
- Jung, M., Koirala, S., Weber, U., Ichii, K., Gans, F., Camps-Valls, G., et al. (2019). The FLUXCOM ensemble of global land-atmosphere energy fluxes. *Scientific Data*, 6(1), 74. <https://doi.org/10.1038/s41597-019-0076-8>
- Keys, P. W., Barnes, E. A., van der Ent, R. J., & Gordon, L. J. (2014). Variability of moisture recycling using a precipitationshed framework. *Hydrology and Earth System Sciences*, 18(10), 3937–3950. <https://doi.org/10.5194/hess-18-3937-2014>
- Keys, P. W., Porkka, M., Wang-Erlandsson, L., Fetzer, I., Gleeson, T., & Gordon, L. J. (2019). Invisible water security: Moisture recycling and water resilience. *Water Security*, 8, 100046. <https://doi.org/10.1016/j.wasec.2019.100046>
- Keys, P. W., van der Ent, R. J., Gordon, L. J., Hoff, H., Nikoli, R., & Savenije, H. H. G. (2012). Analyzing precipitationsheds to understand the vulnerability of rainfall dependent regions. *Biogeosciences*, 9(2), 733–746. <https://doi.org/10.5194/bg-9-733-2012>
- Khanna, J., Medvigy, D., Fueglistaler, S., & Walko, R. (2017). Regional dry-season climate changes due to three decades of Amazonian deforestation. *Nature Climate Change*, 7(3), 200–204. <https://doi.org/10.1038/nclimate3226>
- Lavers, D. A., Ralph, F. M., Waliser, D. E., Gershunov, A., & Dettlinger, M. D. (2015). Climate change intensification of horizontal water vapor transport in CMIP5. *Geophysical Research Letters*, 42(13), 5617–5625. <https://doi.org/10.1002/2015gl064672>
- Lawrence, D., & Vandecar, K. (2015). Effects of tropical deforestation on climate and agriculture. *Nature Climate Change*, 5(1), 27–36. <https://doi.org/10.1038/nclimate2430>
- Li, B., Li, P., Zhang, W., Ji, J., Liu, G., & Xu, M. (2021). Deep soil moisture limits the sustainable vegetation restoration in arid and semi-arid Loess Plateau. *Geoderma*, 399, 115122. <https://doi.org/10.1016/j.geoderma.2021.115122>
- Li, Y., Piao, S., Li, L. Z. X., Chen, A., Wang, X., Ciais, P., et al. (2018). Divergent hydrological response to large-scale afforestation and vegetation greening in China. *Science Advances*, 4(5). <https://doi.org/10.1126/sciadv.aar4182>
- Li, Z., Zheng, F., Liu, W., & Flanagan, D. C. (2010). Spatial distribution and temporal trends of extreme temperature and precipitation events on the Loess Plateau of China during 1961–2007. *Quaternary International*, 226(1–2), 92–100. <https://doi.org/10.1016/j.quaint.2010.03.003>
- Liang, S. (2021). GLASS global land surface satellite leaf area index product [Dataset]. *National Earth System Science Data Center, National Science & Technology Infrastructure of China*. [https://doi.org/10.12041/geodata.GLASS\\_LAI\\_modis\(0.05D\).ver1.db](https://doi.org/10.12041/geodata.GLASS_LAI_modis(0.05D).ver1.db)
- Liu, R., Liu, Y., & Chen, J. (2021). GLOBMAP global leaf area index since 1981 (version 3.0) [Dataset]. *Zenodo*. <https://doi.org/10.5281/zenodo.4700264>
- Liu, W., & Sang, T. (2013). Potential productivity of the Miscanthus energy crop in the Loess Plateau of China under climate change. *Environmental Research Letters*, 8(4), 044003. <https://doi.org/10.1088/1748-9326/8/4/044003>
- Liu, Y., Fu, B., Lü, Y., Wang, Z., & Gao, G. (2012). Hydrological responses and soil erosion potential of abandoned cropland in the Loess Plateau, China. *Geomorphology*, 138(1), 404–414. <https://doi.org/10.1016/j.geomorph.2011.10.009>
- Liu, Y., Ge, J., Guo, W., Cao, Y., Chen, C., Luo, X., et al. (2023). Revisiting biophysical impacts of greening on precipitation over the Loess Plateau of China using WRF with water vapor tracers. *Geophysical Research Letters*, 50(8). <https://doi.org/10.1029/2023gl102809>
- Liu, Y., Xiao, J., Ju, W., Xu, K., Zhou, Y., & Zhao, Y. (2016). Recent trends in vegetation greenness in China significantly altered annual evapotranspiration and water yield. *Environmental Research Letters*, 11(9), 094010. <https://doi.org/10.1088/1748-9326/11/9/094010>
- Lv, M., Ma, Z., & Peng, S. (2019). Responses of terrestrial water cycle components to afforestation within and around the Yellow River basin. *Atmospheric and Oceanic Science Letters*, 12(2), 116–123. <https://doi.org/10.1080/16742834.2019.1569456>
- Miralles, D. G., Holmes, T. R. H., De Jeu, R. A. M., Gash, J. H., Meesters, A. G. C. A., & Dolman, A. J. (2011). Global land-surface evaporation estimated from satellite-based observations. *Hydrology and Earth System Sciences*, 15(2), 453–469. <https://doi.org/10.5194/hess-15-453-2011>
- Naeem, S., Zhang, Y., Zhang, X., Tian, J., Abbas, S., Luo, L., & Meresa, H. K. (2021). Both climate and socioeconomic drivers contribute to vegetation greening of the Loess Plateau. *Science Bulletin*, 66(12), 1160–1163. <https://doi.org/10.1016/j.scib.2021.03.007>
- Piao, S., Wang, X., Park, T., Chen, C., Lian, X., He, Y., et al. (2019). Characteristics, drivers and feedbacks of global greening. *Nature Reviews Earth and Environment*, 1(1), 14–27. <https://doi.org/10.1038/s43017-019-0001-x>
- Ren, Y., Zhang, J., Fu, J., Peng, S., & Li, Z. (2022). Spatiotemporally varied extreme precipitation events simultaneously controlled by multiple circulation factors in China's Loess Plateau. *International Journal of Climatology*, 42(12), 6351–6372. <https://doi.org/10.1002/joc.7593>
- Schneider, U., Becker, A., Finger, P., Meyer-Christoffer, A., Rudolf, B., & Ziese, M. (2015). GPCC full data monthly product version 7.0 at 0.5°: Monthly land-surface precipitation from rain-gauges built on GTS-based and historic data. [https://doi.org/10.5676/DWD\\_GPCC/FD\\_M\\_V7\\_050](https://doi.org/10.5676/DWD_GPCC/FD_M_V7_050)
- Spera, S. A., Galford, G. L., Coe, M. T., Macedo, M. N., & Mustard, J. F. (2016). Land-use change affects water recycling in Brazil's last agricultural Frontier. *Global Change Biology*, 22(10), 3405–3413. <https://doi.org/10.1111/gcb.13298>

- Spracklen, D. V., Arnold, S. R., & Taylor, C. M. (2012). Observations of increased tropical rainfall preceded by air passage over forests. *Nature*, 489(7415), 282–285. <https://doi.org/10.1038/nature11390>
- Spracklen, D. V., Baker, J. C. A., Garcia-Carreras, L., & Marsham, J. H. (2018). The effects of tropical vegetation on rainfall. *Annual Review of Environment and Resources*, 43(1), 193–218. <https://doi.org/10.1146/annurev-environ-102017-030136>
- Staal, A., Flores, B. M., Aguiar, A. P. D., Bosmans, J. H. C., Fetzer, I., & Tuinenburg, O. A. (2020). Feedback between drought and deforestation in the Amazon. *Environmental Research Letters*, 15(4), 044024. <https://doi.org/10.1088/1748-9326/ab738e>
- Staal, A., Tuinenburg, O. A., Bosmans, J. H. C., Holmgren, M., van Nes, E. H., Scheffer, M., et al. (2018). Forest-rainfall cascades buffer against drought across the Amazon. *Nature Climate Change*, 8(6), 539–543. <https://doi.org/10.1038/s41558-018-0177-y>
- Sterling, S. M., Ducharme, A., & Polcher, J. (2012). The impact of global land-cover change on the terrestrial water cycle. *Nature Climate Change*, 3(4), 385–390. <https://doi.org/10.1038/nclimate1690>
- Su, B., & Shangguan, Z. (2018). Decline in soil moisture due to vegetation restoration on the Loess Plateau of China. *Land Degradation and Development*, 30(3), 290–299. <https://doi.org/10.1002/ldr.3223>
- Tan, L., An, Z., Huh, C. A., Cai, Y., Shen, C. C., Shiao, L. J., et al. (2014). Cyclic precipitation variation on the western Loess Plateau of China during the past four centuries. *Scientific Reports*, 4(1), 6381. <https://doi.org/10.1038/srep06381>
- Tang, X., Miao, C., Xi, Y., Duan, Q., Lei, X., & Li, H. (2018). Analysis of precipitation characteristics on the loess plateau between 1965 and 2014, based on high-density gauge observations. *Atmospheric Research*, 213, 264–274. <https://doi.org/10.1016/j.atmosres.2018.06.013>
- Tian, L., Zhang, B., Chen, S., Wang, X., Ma, X., & Pan, B. (2022). Large-scale afforestation enhances precipitation by intensifying the atmospheric water cycle over the Chinese Loess Plateau. *Journal of Geophysical Research: Atmospheres*, 127(16). <https://doi.org/10.1029/2022jd036738>
- Trenberth, K. E. (1999). Atmospheric moisture recycling: Role of advection and local evaporation. *Journal of Climate*, 12(5), 1368–1381. [https://doi.org/10.1175/1520-0442\(1999\)012<1368:AMRROA>2.0.CO;2](https://doi.org/10.1175/1520-0442(1999)012<1368:AMRROA>2.0.CO;2)
- Tuinenburg, O. A. (2013). *Atmospheric effects of irrigation in monsoon climate: The Indian subcontinent*. [Ph.D. Thesis] (p. 179). Wageningen University.
- Tuinenburg, O. A., Bosmans, J. H. C., & Staal, A. (2022). The global potential of forest restoration for drought mitigation. *Environmental Research Letters*, 17(3), 034045. <https://doi.org/10.1088/1748-9326/ac55b8>
- Tuinenburg, O. A., Theeuwes, J. J. E., & Staal, A. (2020). High-resolution global atmospheric moisture connections from evaporation to precipitation. *Earth System Science Data*, 12(4), 3177–3188. <https://doi.org/10.5194/essd-12-3177-2020>
- van der Ent, R. J., & Savenije, H. H. G. (2011). Length and time scales of atmospheric moisture recycling. *Atmospheric Chemistry and Physics*, 11(5), 1853–1863. <https://doi.org/10.5194/acp-11-1853-2011>
- van der Ent, R. J., Savenije, H. H. G., Schaeffli, B., & Steele-Dunne, S. C. (2010). Origin and fate of atmospheric moisture over continents. *Water Resources Research*, 46(9). <https://doi.org/10.1029/2010wr009127>
- van der Ent, R. J., Tuinenburg, O. A., Knoche, H. R., Kunstmann, H., & Savenije, H. H. G. (2013). Should we use a simple or complex model for moisture recycling and atmospheric moisture tracking? *Hydrology and Earth System Sciences*, 17(12), 4869–4884. <https://doi.org/10.5194/hess-17-4869-2013>
- van der Ent, R. J., Wang-Erlandsson, L., Keys, P. W., & Savenije, H. H. G. (2014). Contrasting roles of interception and transpiration in the hydrological cycle – Part 2: Moisture recycling. *Earth System Dynamics*, 5(2), 471–489. <https://doi.org/10.5194/esd-5-471-2014>
- Venables, W. N., & Ripley, B. D. (2002). *Modern applied statistics with S* (4th ed.). <https://doi.org/10.1007/978-0-387-21706-2>
- Wang, S., Fu, B., Piao, S., Lü, Y., Ciais, P., Feng, X., & Wang, Y. (2015). Reduced sediment transport in the Yellow River due to anthropogenic changes. *Nature Geoscience*, 9(1), 38–41. <https://doi.org/10.1038/ngeo2602>
- Wang, X., Wang, B., & Xu, X. (2019). Effects of large-scale climate anomalies on trends in seasonal precipitation over the Loess Plateau of China from 1961 to 2016. *Ecological Indicators*, 107, 105643. <https://doi.org/10.1016/j.ecolind.2019.105643>
- Wang, X., Zhang, B., Li, F., Li, X., Li, X., Wang, Y., et al. (2021). Vegetation restoration projects intensify intraregional water recycling processes in the agro-pastoral ecotone of Northern China. *Journal of Hydrometeorology*. <https://doi.org/10.1175/jhm-d-20-0125.1>
- Wang, X., Zhang, Z., Zhang, B., Tian, L., Tian, J., Arnault, J., et al. (2023). Quantifying the impact of land use and land cover change on moisture recycling with convection-permitting WRF-tagging modeling in the agro-pastoral ecotone of northern China. *Journal of Geophysical Research: Atmospheres*, 128(8), e2022JD038421. <https://doi.org/10.1029/2022JD038421>
- Wang, Y., Liu, X., Zhang, D., & Bai, P. (2023b). Tracking moisture sources of precipitation over China. *Journal of Geophysical Research: Atmospheres*, 128(15), e2023JD039106. <https://doi.org/10.1029/2023JD039106>
- Wang, Z., Fu, B., Wu, X., Li, Y., Feng, Y., Wang, S., et al. (2023). Vegetation resilience does not increase consistently with greening in China's Loess Plateau. *Communications Earth & Environment*, 4(1), 336. <https://doi.org/10.1038/s43247-023-01000-3>
- Wang-Erlandsson, L., Fetzer, I., Keys, P. W., van der Ent, R. J., Savenije, H. H. G., & Gordon, L. J. (2018). Remote land use impacts on river flows through atmospheric teleconnections. *Hydrology and Earth System Sciences*, 22(8), 4311–4328. <https://doi.org/10.5194/hess-22-4311-2018>
- Wierik, S. A., Cammeraat, E. L. H., Gupta, J., & Artzy-Randrup, Y. A. (2021). Reviewing the impact of land use and land-use change on moisture recycling and precipitation patterns. *Water Resources Research*, 57(7). <https://doi.org/10.1029/2020wr029234>
- Wulfmeyer, V., Branch, O., Warrach-Sagi, K., Bauer, H.-S., Schwitalla, T., & Becker, K. (2014). The impact of plantations on weather and climate in coastal desert regions. *Journal of Applied Meteorology and Climatology*, 53(5), 1143–1169. <https://doi.org/10.1175/JAMC-D-13-0208.1>
- Xiao, M., & Cui, Y. (2021). Source of evaporation for the seasonal precipitation in the Pearl River delta, China. *Water Resources Research*, 57(8). <https://doi.org/10.1029/2020wr028564>
- Xmingzh. (2021). xmingzh/Modified-WAM2layers: First release (v1.0.0) [Software]. *Zenodo*. <https://doi.org/10.5281/zenodo.4796962>
- Yang, K., He, J., Tang, W., Lu, H., Qin, J., Chen, Y., & Li, X. (2019). China meteorological forcing dataset (1979–2018). *National Tibetan Plateau / Third Pole Environment Data Center*. <https://doi.org/10.11888/AtmosphericPhysics.tpe.249369.file>
- Yao, Y., Liang, S., Li, X., Hong, Y., Fisher, J. B., Zhang, N., et al. (2014). Bayesian multimodel estimation of global terrestrial latent heat flux from eddy covariance, meteorological, and satellite observations. *Journal of Geophysical Research: Atmospheres*, 119(8), 4521–4545. <https://doi.org/10.1002/2013jd020864>
- Yosef, G., Walko, R., Avisar, R., Tatarinov, F., Rotenberg, E., & Yakir, D. (2018). Large-scale semi-arid afforestation can enhance precipitation and carbon sequestration potential. *Scientific Reports*, 8(1), 996. <https://doi.org/10.1038/s41598-018-19265-6>
- Yu, Y., Zhao, W., Martinez-Murillo, J. F., & Pereira, P. (2020). Loess Plateau: From degradation to restoration. *The Science of the Total Environment*, 738, 140206. <https://doi.org/10.1016/j.scitotenv.2020.140206>
- Zhang, B., Tian, L., Yang, Y., & He, X. (2022). Revegetation does not decrease water yield in the Loess Plateau of China. *Geophysical Research Letters*, 49(9). <https://doi.org/10.1029/2022gl098025>

- Zhang, C., Chen, D., Tang, Q., & Huang, J. (2023). Fate and changes in moisture evaporated from the Tibetan plateau (2000–2020). *Water Resources Research*, 59(11). <https://doi.org/10.1029/2022wr034165>
- Zhang, S., Yang, D., Yang, Y., Piao, S., Yang, H., Lei, H., & Fu, B. (2018). Excessive afforestation and soil drying on China's Loess Plateau. *Journal of Geophysical Research: Biogeosciences*, 123(3), 923–935. <https://doi.org/10.1002/2017JG004038>
- Zhang, S., Yang, H., Yang, D., & Jayawardena, A. W. (2016). Quantifying the effect of vegetation change on the regional water balance within the Budyko framework. *Geophysical Research Letters*, 43(3), 1140–1148. <https://doi.org/10.1002/2015gl066952>